Spontaneous Article

Descriptive anatomy and three-dimensional reconstruction of the skull of the tetrapod *Eoherpeton watsoni* Panchen, 1975 from the Carboniferous of Scotland

Laura B. PORRO[1]*†, Elizabeth MARTIN-SILVERSTONE[2]† and Emily J. RAYFIELD[2]

[1] Centre for Integrative Anatomy, Department of Cell and Developmental Biology, University College London, London, UK.
[2] Palaeobiology Research Group, School of Earth Sciences, University of Bristol, Bristol, UK.
*Corresponding author. E-mail: l.porro@ucl.ac.uk

ABSTRACT: The early tetrapod *Eoherpeton watsoni* is known from the mid- to late Carboniferous (late Viséan to Namurian, approximately 346–313 Ma) of Scotland. The holotype is made up of a nearly complete but crushed skull with postcranial fragments. The skull anatomy of *Eoherpeton* was first described over 40 years ago; however, many details are obscured due to deformation of the specimen, including internal bone surfaces, the palatal bones and dentition, and suture morphology. Most phylogenetic analyses place *Eoherpeton* as an embolomere/reptilomorph on the lineage leading to amniotes, making it a key taxon for understanding anatomical changes during the fish-tetrapod transition. In this paper, we scanned the holotype using micro-computed tomography and digitally prepared the specimen. Based on these data, we present a revised description of the skull, including sutural morphology, that supplements and amends previous descriptions. New anatomical findings include the presence of a previously unknown tooth-bearing vomer, additional information on the shape of the basipterygoid processes and jaw joint, the ability to visualise the full extent of the pterygoid, and confirmation of the arrangement of the coronoid series. We also note the size of the pterygoid flange, which is larger than previously described for *Eoherpeton*. The pterygoid flange is widely considered to be characteristic of amniotes and serves as the origin of the medial pterygoideus muscle. The differentiation of the adductor muscles and appearance of medial pterygoideus are thought to have permitted a static pressure bite in amniotes, potentially resulting in greater bite forces and increased dietary range. Thus, the presence and extent of the pterygoid flange in *Eoherpeton* suggests this feature (and associated changes in feeding mechanism) may have evolved earlier than previously thought. Finally, the skull was digitally repaired and retrodeformed to create a new, hypothetical three-dimensional reconstruction of the skull of *Eoherpeton*.

KEY WORDS: computed tomography, cranium, embolomeres, mandible, retrodeformation, sutures.

The fish–tetrapod transition has long been an area of intense focus in palaeontology and evolutionary biology (Ahlberg & Milner 1994; Laurin *et al*. 2000; Clack 2006, 2009, 2012), in part due to the number of profound anatomical changes needed to adapt to terrestrial environments, such as changing from breathing water to air (Janis & Farmer 1999; Janis & Keller 2001; Graham *et al*. 2014) and from swimming to walking on land (Daeschler *et al*. 2006; Shubin *et al*. 2006; Boisvert *et al*. 2008; Pierce *et al*. 2012; Molnar *et al*. 2018). Feeding was also affected during the water–land transition, with a presumed shift from using suction feeding – expanding the oral cavity and generating a pressure differential to capture and ingest prey (Wainwright *et al*. 2015) – to biting and snapping (Heiss *et al*. 2018; Van Wassenberg 2019). This shift in feeding mechanism required changes to head and skull anatomy, including overall skull shape, kinetic potential, jaw opening and closing musculature, and dentition. Previous studies of early tetrapod skulls have focused on whether individual taxa exhibit anatomical features linked to either suction feeding or biting (Clack 2012; Anderson *et al*. 2013; Neenan *et al*. 2014; Porro *et al*. 2015a, 2015b; Rawson *et al*. 2021; Deakin *et al*. 2022), although notably some taxa appear to have maintained suction-feeding while simultaneously developing elaborate mechanisms for bite-based prey capture (Lemberg *et al*. 2021). Understanding this transition requires integrating numerous aspects of skull anatomy in presumably fully aquatic, amphibious and fully terrestrial early tetrapod taxa.

Watson (1929) described a small skull (formerly known as specimen number RSM GY 1950.86.1, now known as NMS

†Joint first authors.

 doi:10.1017/S175569102300018X

G.1950.86.1, where NMS is the institutional abbreviation for National Museums of Scotland, Edinburgh, United Kingdom), which he attributed to *Pholidogaster pisciformis* (Huxley 1862; Fig. 1). The skull had no associated data, but based on the nature of the matrix, Watson (1929) suggested it was from the Upper Viséan (Lower Carboniferous) Gilmerton Ironstone at Gilmerton (near Edinburgh), Scotland. Panchen (1975) later conducted analyses of the matrix, which supported this provenance; however, new preparation techniques applied to the specimen led him to identify it as a new genus and species, *Eoherpeton watsoni* (Panchen 1975), an anthracosaur. More recent studies have placed *E. watsoni* as an embolomere or reptilomorph on the lineage leading to amniotes (Klembara *et al*. 2010; Clack 2012). The specimen comprises a nearly complete but crushed skull along with fragmentary postcranial elements. The skull roof, right side of the facial skeleton, and lateral side of the right lower jaw are well preserved and visible in dorsal view; the medial side of the right lower jaw, much of the palate, portions of the braincase, and the less-well-preserved left side of the facial skeleton and left lower jaw are visible in ventral view. The skull was described in detail by Panchen (1975) and was later revisited by Smithson (1985), who also identified additional material of *E. watsoni* from a Namurian locality near Cowdenbeath in the Fife Coalfield (Smithson 1980). Both Panchen (1975) and Smithson (1985) used available materials to produce two-dimensional reconstructions of the skull of *E. watsoni* in multiple views, which differed in several aspects from each other.

Fossil material is typically preserved damaged and deformed, and restoring fossils to their original shape has a long history within palaeontology and palaeoanthropology. Such restorations are vital for deciphering the life appearance and potential ecology of organisms (Lautenschlager 2017), the application of subsequent analytical techniques such as geometric morphometrics (Felice *et al*. 2020) and biomechanical modelling (Rayfield 2007; Pierce *et al*. 2012; Demuth *et al*. 2023), and for deciphering taxonomic placement and phylogenetic position. Reconstructions of fossil skulls have historically been performed using photographs, drawings or plaster models (Davis & Napier 1963). Medical imaging methods, particularly computed tomography (CT) and micro-computed tomography (μCT) scanning, have revolutionised the study of fossil organisms (Conroy & Vannier 1984; Cunningham *et al*. 2014; Rahman & Smith 2014). Over the past decades, increasingly sophisticated techniques have been developed to digitally repair damage and deformation to create virtual three-dimensional (3D) reconstructions of fossil skulls (Zollikofer *et al*. 1995; Motani 1997; Gunz *et al*. 2009; Lautenschlager 2016), including early tetrapod skulls (Porro *et al*. 2015a, 2015b, 2023; Pardo *et al*. 2017; Lemberg *et al*. 2021; Rawson *et al*. 2021; Arbez *et al*. 2022). In this study, we use μCT and visualisation software to digitally prepare the type specimen of *E. watsoni*, revealing new anatomical details that supplements previous descriptions (Watson 1929; Panchen 1975; Smithson 1985). Individual skull bones were then manipulated to produce a new 3D digital model of the morphology of the skull of *E. watsoni.*

1. Material and methods

The holotype specimen of *E. watsoni,* NMS G.1950.86.1, was μCT scanned at the Imaging and Analysis Centre of the Natural History Museum (London, UK) on a Nikon XT H 225 μCT scanner (Nikon Metrology, Tring, UK). The specimen was scanned at 210 kV and 240 μA with a 1.5-mm-thick copper filter, 500 ms exposure, 3142 projections with one frame per projection. Reconstruction produced 1995 transverse slices with a voxel size of 0.0918 mm/voxel. Original CT data for the specimen are available on MorphoSource (https://www.morphosource.org/concern/media/000598394?locale=en). CT scans were processed using the visualisation software Avizo 7.1.1–9.5 and Amira 6.7.0 – Amira 3D 2021.1 (Thermo Fisher Scientific, Waltham, Massachusetts, USA). Within the Segmentation Editor, density thresholding was used to initially separate bone from matrix. Scans were then processed slice-by-slice (interpolating across no more than five slices at a time) to separate individual bones and teeth from each other (Fig. 2). Sutures typically present as low-density areas between bones, although occasionally high-density minerals precipitate within them. Photographs and line drawings of the original specimen were used to confirm the location of sutures and differentiate them from post-mortem damage. Three-dimensional surface models (.surf files) of individual bones and teeth were created and could be manipulated in 3D space; the following description is based on these models (Supplementary Figs 1–11 available at https://doi.org/10.1017/S175569102300018X). Some surfaces were subsequently exported to the software Blender (Amsterdam, Netherlands) to create the final main text and supplementary figures.

Some limits to the data set used in the description and 3D reconstruction should be noted. Although scan resolution was comparable to those in previous descriptions of *Acanthostega* and *Crassigyrinus* (Porro *et al*. 2015b, 2023), contrast between individual bones was sometimes too poor to clearly discern suture morphology, although contacts were usually clear (with the exception of the contacts between the squamosal–quadrate–quadratojugal and the dentary–coronoid series; see details below). We clearly acknowledge any uncertainties in the nature of contacts between elements in the following description; future synchrotron scanning of *E. watsoni* could potentially resolve these ambiguities. NMS G.1950.86.1 has been asymmetrically deformed, resulting in the skull roof and right side of the upper and lower jaws dorsally overlying the palate and left side of the skull. The left side of the facial skeleton is less well preserved than the right side, although it still yielded anatomical data and was useful in the 3D reconstruction. The posterior

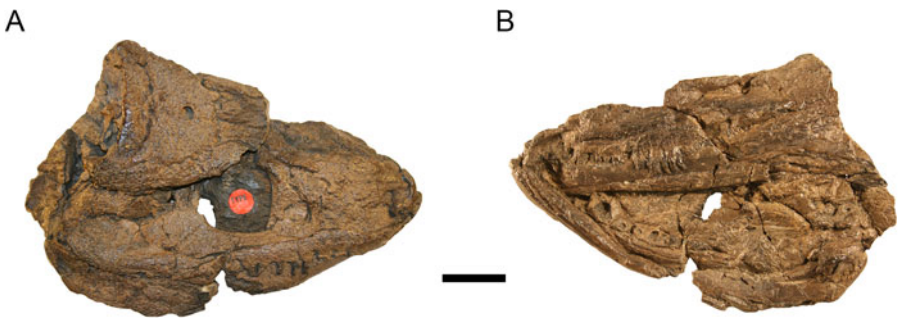

Figure 1 Type specimen of *Eoherpeton watsoni*, NMS G.1950.86. (A) Specimen in dorsal/right lateral view. (B) Specimen in ventral/left lateral view. Photographs by Stig Walsh. Scale bar = 30 mm. Abbreviation: NMS = National Museums of Scotland, Edinburgh, United Kingdom.

https://doi.org/10.1017/S175569102300018X Published online by Cambridge University Press

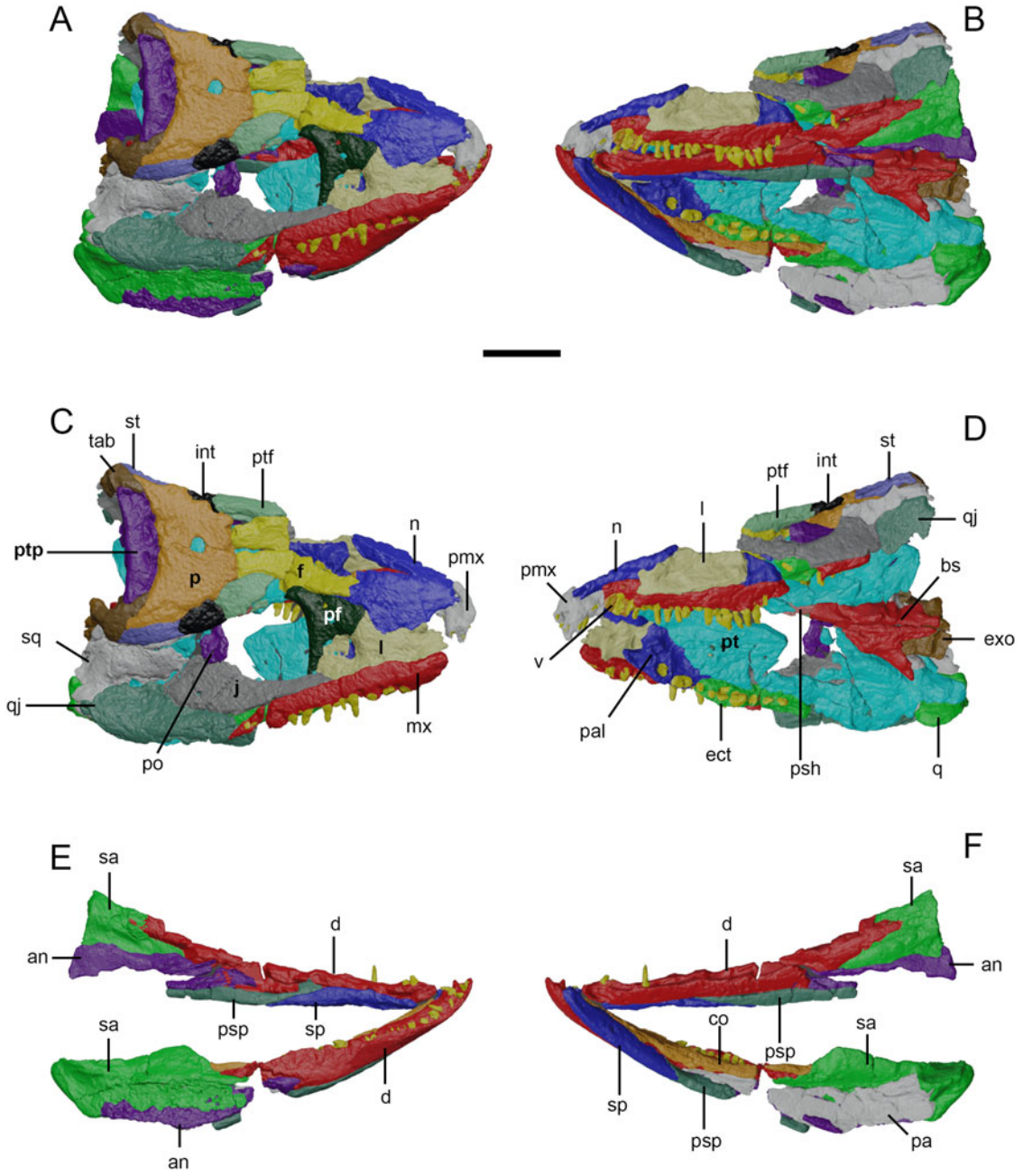

Figure 2 Surface models of *Eoherpeton watsoni*, NMS G.1950.86 from micro-computed tomography data. Matrix, postcranial bones and bones of uncertain identity have been removed. Individual bones are shown in different colours. (A) Upper and lower jaws in dorsal/right lateral view. (B) Upper and lower jaws in ventral/left lateral view. (C) Upper jaw in dorsal/right lateral view with individual bones labelled. (D) Upper jaw in dorsal/right lateral view with individual bones labelled. (E) Lower jaws in dorsal/right lateral view with individual bones labelled. (F) Lower jaws in dorsal/right lateral view with individual bones labelled. Abbreviations: NMS = National Museums of Scotland, Edinburgh, United Kingdom; an = angular; bs = basisphenoid; co = coronoid (anterior, middle, and posterior); d = dentary; ect = ectopterygoid; exo = exoccipital; f = frontal; int = intertemporal; j = jugal; l = lacrimal; mx = maxilla; n = nasal; p = parietal; pa = prearticular; pal = palatine; pf = prefrontal; pmx = premaxilla; po = postorbital; psh = parasphenoid; psp = postsplenial; pt = pterygoid; ptf = postfrontal; ptp = postparietal; q = quadrate; qj = quadratojugal; sa = surangular; sp = splenial; sq = squamosal; st = supratemporal; tab = tabular; v = vomer. Scale bar = 30 mm.

portion of the left lower jaw ramus is severely crushed and the region of the jaw joint is missing. The frontals and nasals have been fractured, and the right squamosal has been preserved in several large pieces. The right lower jaw ramus was broken at its midpoint, and small portions of the right splenial, postsplenial, angular and prearticular are missing, although the left postsplenial preserves the area that was lost on the right side. The anterior end of the right dentary has been deformed about its long axis so that the tooth row is twisted outwards. The right lower jaw ramus contains a well-preserved and articulated jaw joint; however, due to complete fusion, the contact between articular and surangular cannot be distinguished. Additionally, the full length of the contact between the right coronoid series and the dentary could not be traced with confidence. In general, the skull has undergone simple fracturing rather than plastic deformation, though there may be some plastic deformation in the palate and anterior right lower jaw, which will be discussed further below. The basisphenoid and parasphenoid are relatively well preserved and an element identified here as the right exoccipital is distinct from surrounding matrix and bones (see more in Section 2.4).

Most 3D reconstructions of early tetrapod skulls are based on well-preserved individual specimens (Porro *et al.* 2015a; Lautenschlager *et al.* 2016; Fortuny *et al.* 2017; Arbez *et al.* 2022), with rarer attempts made to reconstruct skulls exhibiting more pronounced deformation (Porro *et al.* 2015b, 2023; Rawson

https://doi.org/10.1017/S175569102300018X Published online by Cambridge University Press

et al. 2021). Reconstruction of the skull of *E. watsoni* was based primarily on bones from the right side and midline of NMS G.1950.86.1, although the left vomer and its teeth were used because of the apparent absence of this element on the right, and a portion of the left pterygoid preserving the basal articulation was merged with the right pterygoid. With the exception of single median elements (basisphenoid, parasphenoid), all bones were reflected across midline to create the left side of the skull.

Using the Transform Editor within Avizo/Amira, the well-preserved right-side palatal elements (palatine, ectopterygoid and pterygoid) were assembled around the midline basisphenoid and parasphenoid; the palate was initially oriented horizontally, establishing a maximum possible width for the skull. The cranium was built upwards by fitting the right-side facial bones together at sutural contacts, finishing with the skull roof. Throughout retrodeformation, the elements were constantly adjusted as more information was gained. This resulted in an initial 3D reconstruction that contained several discrepancies, including poor contact between the lateral margins of the skull roof and facial bones, no contact between quadrate and the quadratojugal (laterally) or pterygoid (medially), and intersection of the pterygoid flange and surangular. These issues were corrected by moderate dorsal vaulting of the palate, resulting in an angle of approximately 102° between the horizontal laminae of the left and right pterygoids, and subsequent shifting of other cranial bones. Although early tetrapods have traditionally been reconstructed with horizontal palates, the presence of a dorsally vaulted palate in *E. watsoni* as well as *Acanthostega* (Porro *et al*. 2015b), *Ichthyostega* (Rosen *et al*. 1981), *Crassigyrinus* (Porro *et al*. 2023) and *Whatcheeria* (Bolt & Lombard 2018; Rawson *et al*. 2021) suggests that this assumption needs serious reconsideration. As a result of some degree of plastic deformation in the dentary and prearticular bones of the right lower jaw, these elements were segmented in several pieces to remove deformation. The intramandibular angle of the reconstructed lower jaws (21.3° measured from the symphysis to the posterior tips of the surangulars) was determined by fitting together the anterior ends of the rami at the symphysis; the right jaw joint (articular-quadrate) that was used to reconstruct both rami is well preserved and articulated.

Unrepaired 3D models of the upper and lower jaws are shown in Figures 3 and 4. A final model (Fig. 5) was produced by repairing breaks and holes in individual bones using interpolation. It should be noted that a few bones, including the missing posterior part of the premaxilla, squamosal, postorbital, and quadrate ramus of the pterygoid in the upper jaw, as well as the postsplenial and angular in the lower jaw, required more extensive reconstruction. Three-dimensional models of the reconstructed upper and lower jaws are available for inspection (Supplementary 3D PDFs 1 and 2). Transformation matrices for all skull bones from the original CT data set to the final 3D reconstructed model are also available (Supplementary Text). This 3D model represents our best hypothesis of the shape of the *E. watsoni* skull based on bones preserved in the type specimen, scan resolution and personal interpretation. We also created interpretive line drawings of the skull from our final 3D model to clearly visualise bone boundaries and areas of uncertainty (Fig. 6).

2. Anatomical description

As previously noted, the present work is not intended as a detailed redescription of the skull of *E. watsoni,* which has been extensively described by Panchen (1975) and Smithson (1985). Instead, we focus on anatomical features visible in CT scans.

2.1. Facial skeleton and cheek

The right premaxilla is better preserved than the left element (Figs 2, 3 and Supplementary Fig. 1), although both its posterior (articulation with the maxilla) and anteromedial (articulation with its counterpart at the midline) margins have been eroded. In transverse section, the premaxilla is gently laterally bowed and mediolaterally widest at the alveolar margin. Scans reveal two complete teeth and fragments of two additional teeth in the right maxilla; however, there is a large gap and what appears to be an empty alveolus between the first and third teeth, as well as an isolated tooth preserved in the matrix medial to this position. Portions of four teeth are visible in the left premaxilla as well as the alveolus noted by Panchen (1975). It would appear there were five premaxillary teeth in *E. watsoni*; however, as previously noted, the posterior end of the premaxilla (including the alveolar margin) is missing, and it is possible that the original tooth count was higher. The premaxillary teeth are slender, recurved in lateral view and straight in anterior view. The more fragmentary left premaxilla preserves the dorsoventrally tall butt joint that presumably contacted the right premaxilla across the midline, and the right element preserves the curved anterior process that anteriorly demarcates the external naris; its rounded tip fits into a clear groove at the anterior margin of the nasal, although this joint has opened in this specimen. CT scans reveal that the mass of bone visible within the right external naris is almost certainly part of the left dentary, not the septomaxilla as identified by Panchen (1975). The premaxilla–maxilla contact is disrupted on the right side, but the posterodorsal corner of the left premaxilla laterally overlaps the anterior edge of the maxilla. The medial aspect of the left premaxilla also makes an anteroposteriorly short, curved contact with the anterolateral aspect of the vomer. There is no distinct medial premaxillary shelf on either side. Reconstructions of the palate by both Panchen (1975) and Smithson (1985) illustrate an uncertain point contribution of the premaxilla to the margin of the internal naris. Our 3D reconstruction (Fig. 3C) suggests the premaxilla reached the choana; however, due to the incomplete preservation of the premaxilla, this contribution is uncertain.

In dorsal view (Figs 3B, 5C) the internarial region is narrower in our reconstruction than in those of Panchen (1975) and Smithson (1985). As noted previously, the anteromedial margin of the right premaxilla is slightly eroded and it is possible that this area was mediolaterally wider in life although it seems unlikely it was as wide as in these previous reconstructions.

We could not identify a septomaxilla in scans of NMS G.1950.86 (as previously discussed, the mass of bone identified by Panchen [1975] as the septomaxilla is in fact part of the left dentary). We clarify that the mass of bone seen within the external naris of our reconstruction in lateral view (Figs 3A, 5A) is in fact the vomer, not a septomaxilla.

The maxilla (Figs 2, 3 and Supplementary Fig. 1) is preserved and broken on both sides of NMS G.1950.86, with the right element being more complete although its anterior margin is missing, as previously noted by Panchen (1975) and Smithson (1985). In transverse section the maxilla is laterally convex; anteriorly, it is rounded in cross-section whereas posteriorly it is mediolaterally expanded at the alveolar margin and thins dorsally. There is a pronounced medial maxillary shelf immediately above the tooth row along the full length of the element. The maxillary teeth are slightly recurved in lateral view, slightly medially curved in anterior view, and bluntly pointed. The middle maxillary teeth are the largest and the posterior maxillary teeth are the smallest. There are 15 teeth preserved in the right maxilla and 25 teeth preserved in the left maxilla, with no distinct empty alveoli. Both Panchen (1975) and Smithson (1985) illustrate an uncertain point contribution of the maxilla to the ventral margin of the external naris. Our

https://doi.org/10.1017/S175569102300018X Published online by Cambridge University Press

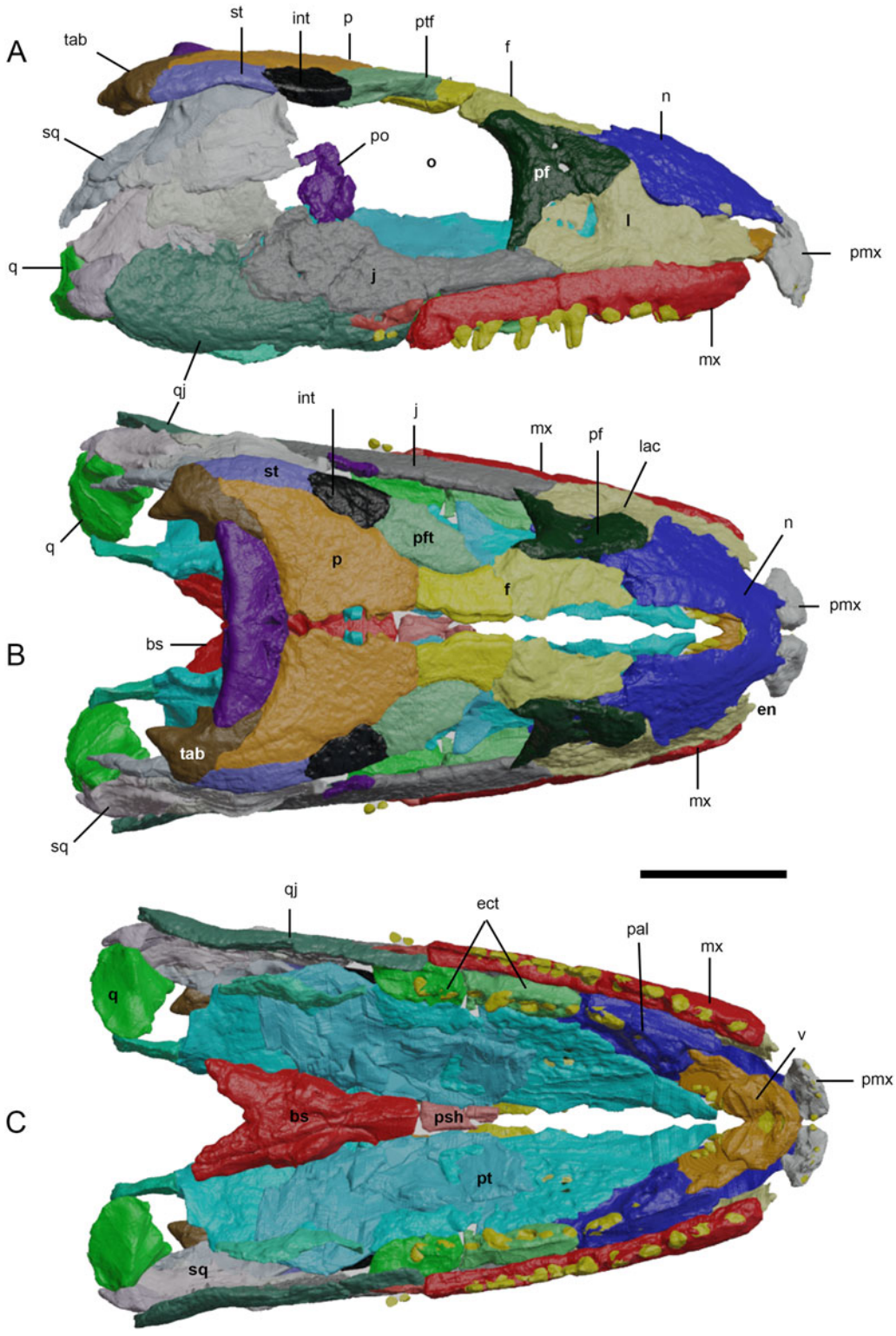

Figure 3 Three-dimensional reconstruction of the cranium of *Eoherpeton watsoni* before repair. Individual bones are shown in different colours; individual fragments of the same bone are shown in slightly different shades. (A) Right lateral view. (B) Dorsal view. (C) Ventral view. Abbreviations: bs = basisphenoid; ect = ectopterygoid; en = external naris; f = frontal; int = intertemporal; j = jugal; l = lacrimal; mx = maxilla; n = nasal; o = orbit; p = parietal; pal = palatine; pf = prefrontal; pmx = premaxilla; po = postorbital; psh = parasphenoid; pt = pterygoid; ptf = postfrontal; ptp = postparietal; q = quadrate; qj = quadratojugal; sq = squamosal; st = supratemporal; tab = tabular; v = vomer. Scale bar = 30 mm.

3D reconstruction (Figs 3, 5) also suggests that if the maxilla reached the external naris, its contribution was limited. The dorsal edge of the maxilla shares long contacts with both the lacrimal and jugal. Anteriorly, the ventral margin of the lacrimal laterally overlaps the dorsal margin of the maxilla; posteriorly, this contact grades into a rounded butt joint. The contact between the maxilla and jugal has been disrupted on both sides but the preserved bone margins suggest these bones contacted at a grooved butt joint. The tapering posterior process of the maxilla laterally overlaps the quadratojugal, excluding the jugal from the ventral skull margin as noted by Panchen (1975). Reconstructions by Panchen (1975) and Smithson (1985) as well as our 3D reconstruction suggest that the maxilla formed the lateral wall of the choana, but there is no evidence from any of these three reconstructions that the maxilla reached the vomer. The lateral margins of the palatine and ectopterygoid contact the

https://doi.org/10.1017/S175569102300018X Published online by Cambridge University Press

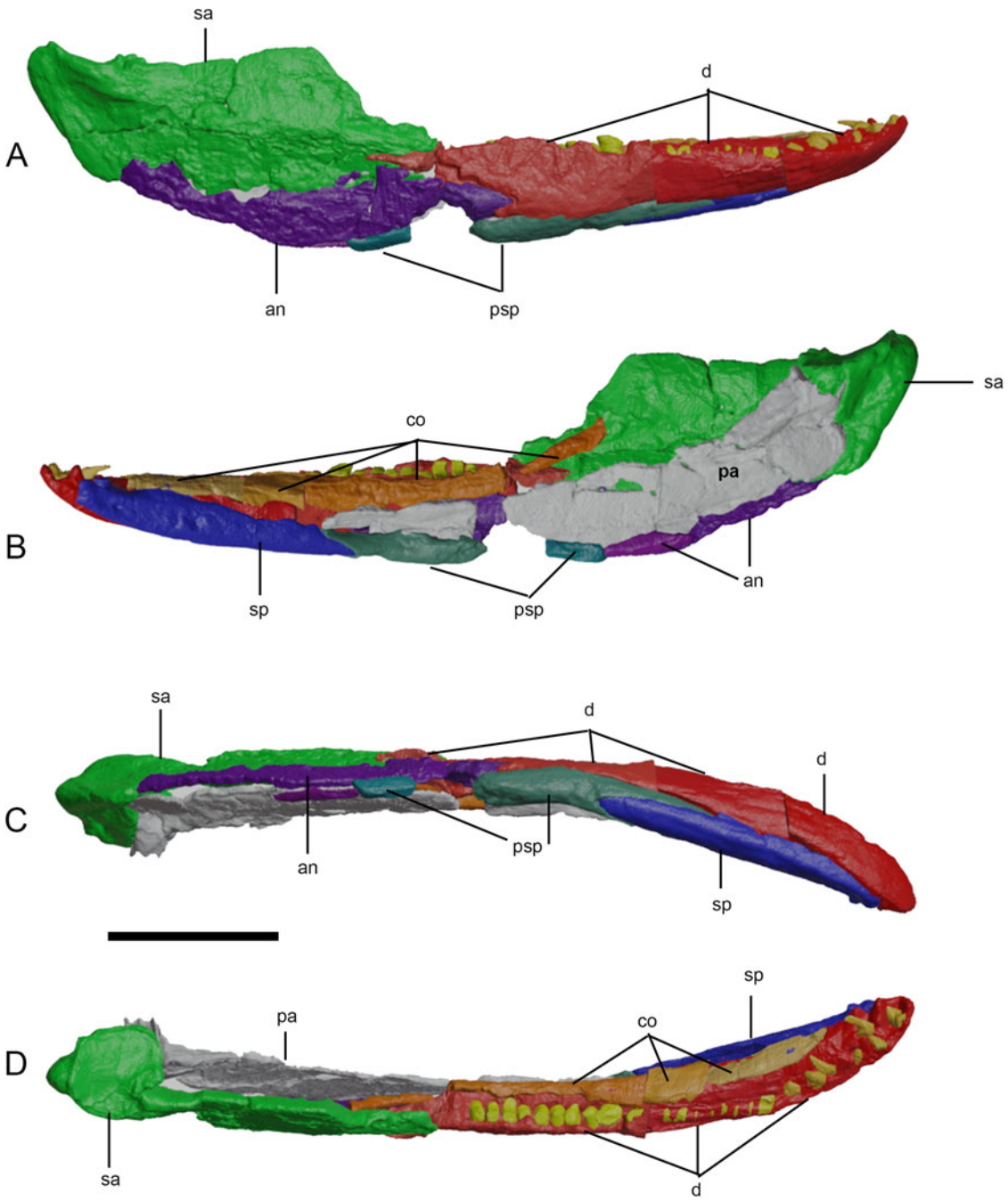

Figure 4 Three-dimensional reconstruction of the right lower jaw of *Eoherpeton watsoni* before repair. Individual bones are shown in different colours; individual fragments of the same bone are shown in slightly different shades. (A) Lateral view. (B) Medial view. (C) Ventral view. (D) Dorsal view. Abbreviations: an = angular; co = coronoid (anterior, middle, and posterior); d = dentary; pa = prearticular; psp = postsplenial; sa = surangular; sp = splenial. Scale bar = 30 mm.

medial aspect of the maxilla, fitting dorsal to the maxillary shelf; faint interdigitations are visible at the right maxilla–palatine contact.

The lacrimal (Figs 2, 3 and Supplementary Fig. 2) is preserved on both sides of NMS G.1950.86 although the left element is missing its dorsal process. The anterior and central portions of the lacrimal exhibit a uniform thickness in transverse section; posteriorly, it is mediolaterally widest ventrally and thins dorsally. The ragged anterior margin of the lacrimal forms the posterior border of the external naris. The lacrimal closely approaches but does not reach the orbit, being excluded by a short contact between the prefrontal and jugal. The lateral surface of the lacrimal ventral and just anterior to the dorsal process is depressed on both sides of the specimen. The dorsal margin of the bone anterior to the dorsal process is smoothly emarginated and is laterally and dorsally overlapped by the nasal in a wide, curving contact, with the dorsal process of the lacrimal inserting between the nasal and prefrontal. The ventral edge of the prefrontal laterally overlapped the posterodorsal margin of the lacrimal, whereas the posteroventral margin of the lacrimal contacted the jugal at a mediolaterally wide butt joint. Faint interdigitations may be present at the latter contact but this is uncertain due to poor scan contrast. Due to deformation of the specimen, the medial aspect of the lacrimal makes broad contact with the dorsal aspect of the palatine; however, this is an artefact. The 3D reconstruction suggests that the ventromedial edge of the lacrimal may have had limited contact with the dorsolateral edge of the palatine but this contact was far less extensive in *E. watsoni* than in *Crassigyrinus* (Porro *et al.* 2023).

https://doi.org/10.1017/S175569102300018X Published online by Cambridge University Press

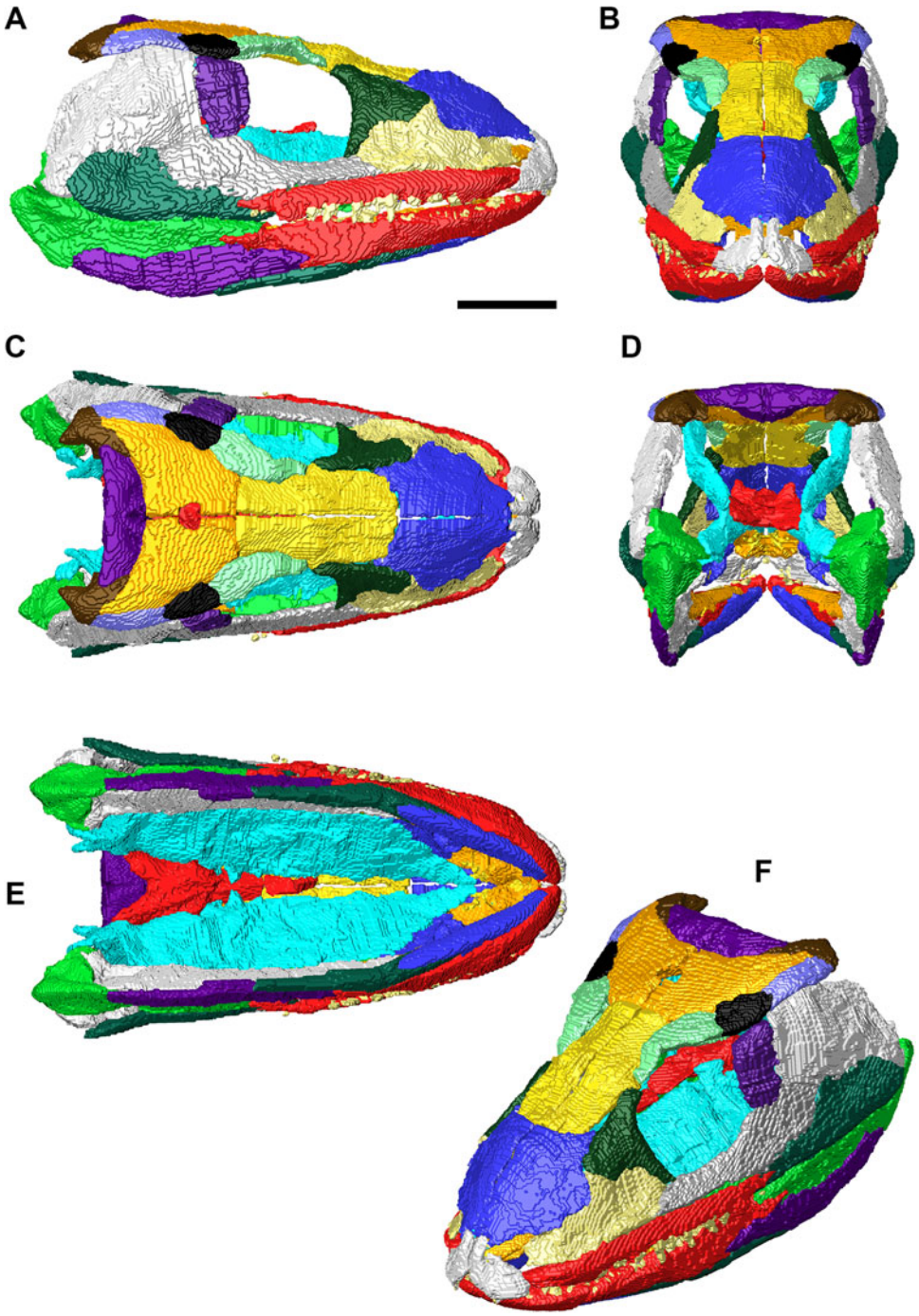

Figure 5 Final three-dimensional reconstruction of the skull of *Eoherpeton watsoni* after repair. Individual bones are shown in different colours following Figures 3 and 4. (A) Right lateral view of upper and lower jaws. (B) Anterior view of upper and lower jaws. (C) Dorsal view of upper and lower jaws. (D) Posterior view of upper and lower jaws. (E) Ventral view of upper and lower jaws. (F) Upper and lower jaws in dorsolateral oblique view. Scale bar = 30 mm; no scale bar for oblique view.

Due to the incomplete posterior margin of the right premaxilla, the incomplete anterior margin of the right maxilla, and the potentially incomplete anterior margin of the lacrimal, as well as extensive crushing in the region, there are uncertainties in our reconstruction of the external naris of *E. watsoni*. Our reconstructed naris is proportionately larger than those of other embolomeres for which skull reconstructions exist (Romer 1963, 1970); additionally, while the nares of other taxa are rounded, the naris of *E. watsoni* in our reconstruction is triangular. It is possible that the missing margins of the premaxilla, maxilla and, potentially, lacrimal may have resulted in the external naris being smaller and more rounded in life than in our reconstruction. We note, however, that the pattern of bones forming the margins of the external naris (the premaxilla forming the anterior margin, the nasal forming the dorsal margin, the lacrimal forming the posterior margin and the premaxilla – and possibly maxilla – forming the ventral margin) is consistent with the pattern seen in other embolomeres (Romer 1963, 1970).

The right jugal (Figs 2, 3 and Supplementary Fig. 2) is complete whereas only the anterior part of the left jugal is visible in the specimen; however, CT scans reveal that the left element is also nearly complete and largely hidden deep to the left quadratojugal (Supplementary Fig. 2F). In transverse section the anterior jugal is robust and square in cross-section; posteriorly, the bone increases in dorsoventral height and thins mediolaterally, with the ventral margin being mediolaterally wider than the dorsal margin. The anterior process tapers to a fine point

https://doi.org/10.1017/S175569102300018X Published online by Cambridge University Press

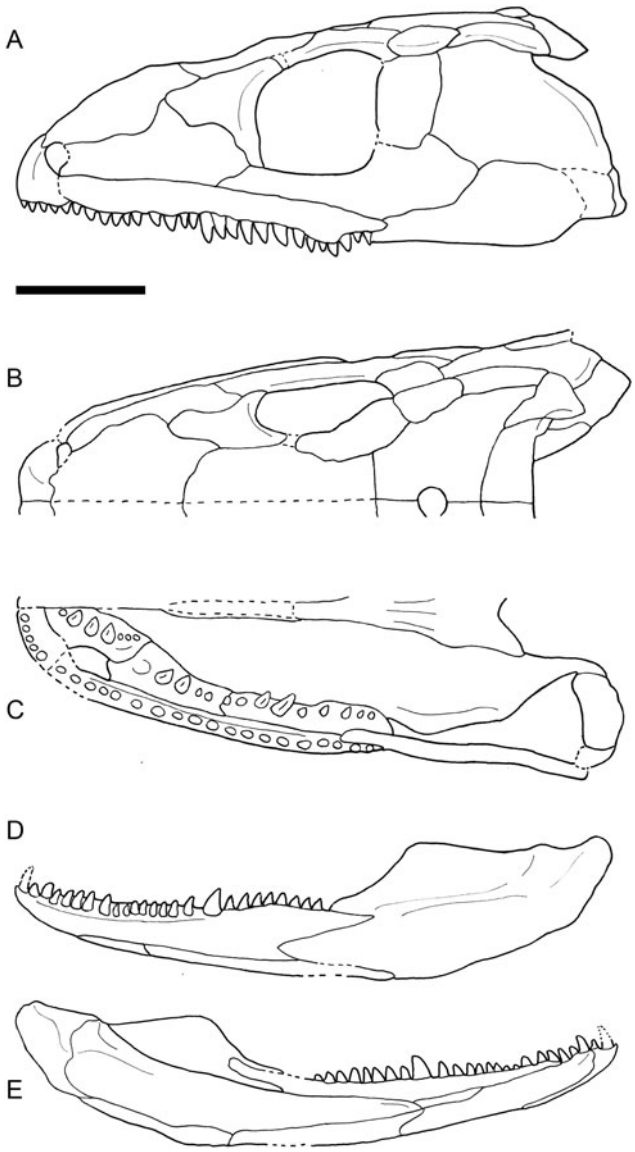

Figure 6 Line drawings of the three-dimensional reconstruction of the skull of *Eoherpeton watsoni* after repair, showing contacts between bones, dentition and major skull openings. (A) Left lateral view of the cranium. (B) Dorsal view of right side. (C) Ventral view of right side. (D) Lateral view of left lower jaw ramus. (E) Medial view of left lower jaw ramus. Dotted lines indicate areas of uncertainty or inferred features/contacts. Scale bar = 30 mm.

that inserts between the maxilla and the lacrimal. Just anterior to the orbital margin, the jugal has a short butt contact with the prefrontal that excludes the lacrimal from the orbit. The contact between the jugal and postorbital appears to have been a simple butt joint, with the postorbital nestled into a distinct notch in the dorsal margin of the jugal. The posteroventral margin of the jugal is laterally overlapped by the dorsal margin of the quadratojugal. The contact between the jugal and squamosal has opened on the right side; the left side suggests the ventral margin of the squamosal laterally overlapped the posterodorsal margin of the jugal, but it should be noted that many elements in this area have been displaced. The ventromedial margin of the anterior two-thirds of the jugal are gently excavated and it seems likely that this surface contacted the dorsolateral margins of the palatine and ectopterygoid. However, the degree of contact between these surfaces is now greatly exaggerated due to deformation of the specimen.

Only a fragment of the dorsal margin of the left squamosal of NMS G.1950.86 is preserved; in contrast, most of the right squamosal is present although it has been broken into at least six separate pieces, some of which overlie each other (Figs 2, 3 and Supplementary Fig. 3). The bone forms the posterodorsal margin of the upper jaw; anteriorly, this margin curves dorsally to meet the skull roof, which it meets in a complex suture (see below). The anterior and ventral margins are now damaged but appear to have originally formed a continuous, rounded curve that articulated with many of the cheek bones. In transverse section, the right squamosal is laterally bowed; it is mediolaterally thinnest ventrally and expands dorsally at its contact with the skull roof. The contact with the postorbital is not preserved; the anterodorsal margin of the squamosal is inturned and gently grooved to articulate with the bones of the skull roof. Based on scans, previous reconstructions (Panchen 1975; Smithson 1985) and the new 3D reconstruction, the dorsal margin of the squamosal contacted the ventrolateral aspect of the supratemporal and posteroventral corner of the intertemporal. Panchen (1975) identified a groove along the thickened posterior border of the squamosal as the border of the otic notch, anchoring the tympanum; Smithson (1985) suggested instead that this groove was the site of origin of the musculus depressor mandibulae. Scans reveal that the medial aspect of the posterodorsal margin of the squamosal features a second distinct groove anteriorly, which flattens posteriorly, and presumably articulated with the vertical quadrate wing of the pterygoid, although no part of this contact survives.

Panchen (1975) initially reconstructed the skull with a long, posteroventral process of the squamosal extending posterior to the quadratojugal. Smithson (1985) pointed out that such an arrangement had not been seen previously in early tetrapods and, after further preparation, suggested that Panchen (1975) had misinterpreted a vertical crack in the quadratojugal as part of the squamosal–quadratojugal contact. Instead, Smithson (1985) reconstructed a more typical arrangement in which the squamosal and quadratojugal form the posterodorsal and posteroventral margins of the skull, respectively, and the quadratojugal medially contacts the quadrate. This area is difficult to interpret in our scans, as illustrated in Figure 7. Anteriorly (Fig. 7C), the dorsal margin of the quadratojugal laterally overlaps the ventral margin of the squamosal. At the level of the anterior edge of the quadrate (Fig. 7D), a distinct and unbroken piece of bone appears, which rapidly expands dorsoventrally (Fig. 7E). This sheet of bone contacts a piece of the squamosal dorsally at a very tight joint. Its ventral margin is laterally overlapped by the dorsal margin of the main piece of the quadratojugal. Moving posteriorly, the ventral margin of this piece of bone expands mediolaterally and flattens, being continuous with the articular surface of the quadrate and forming part of the jaw joint of *E. watsoni* (Fig. 7F). The concave medial surface of this sheet of bone broadly contacts the lateral surface of the quadrate.

We originally identified this piece of bone as a portion of the squamosal (Fig. 7G), based on its very tight junction with a definitive piece of the squamosal dorsal to it (Fig. 7E) and a more open contact with the overlapping quadratojugal ventral to it; this open contact is continuous with the gap between the quadratojugal and surangular of the lower jaw. However, such an arrangement would be unusual in several respects: the squamosal would insert between the quadrate and quadratojugal, preventing contact between these elements; the squamosal would form the posteroventral margin of the upper jaw instead of the quadratojugal; and the squamosal would form part of the jaw joint. Alternatively, the piece could belong to the quadratojugal (Fig. 7H), which would result in direct contact between the medial aspect of the quadratojugal and lateral aspect of the quadrate, as well as the quadratojugal contributing to the jaw joint, and a more typical arrangement of bones as seen in other early tetrapods.

https://doi.org/10.1017/S175569102300018X Published online by Cambridge University Press

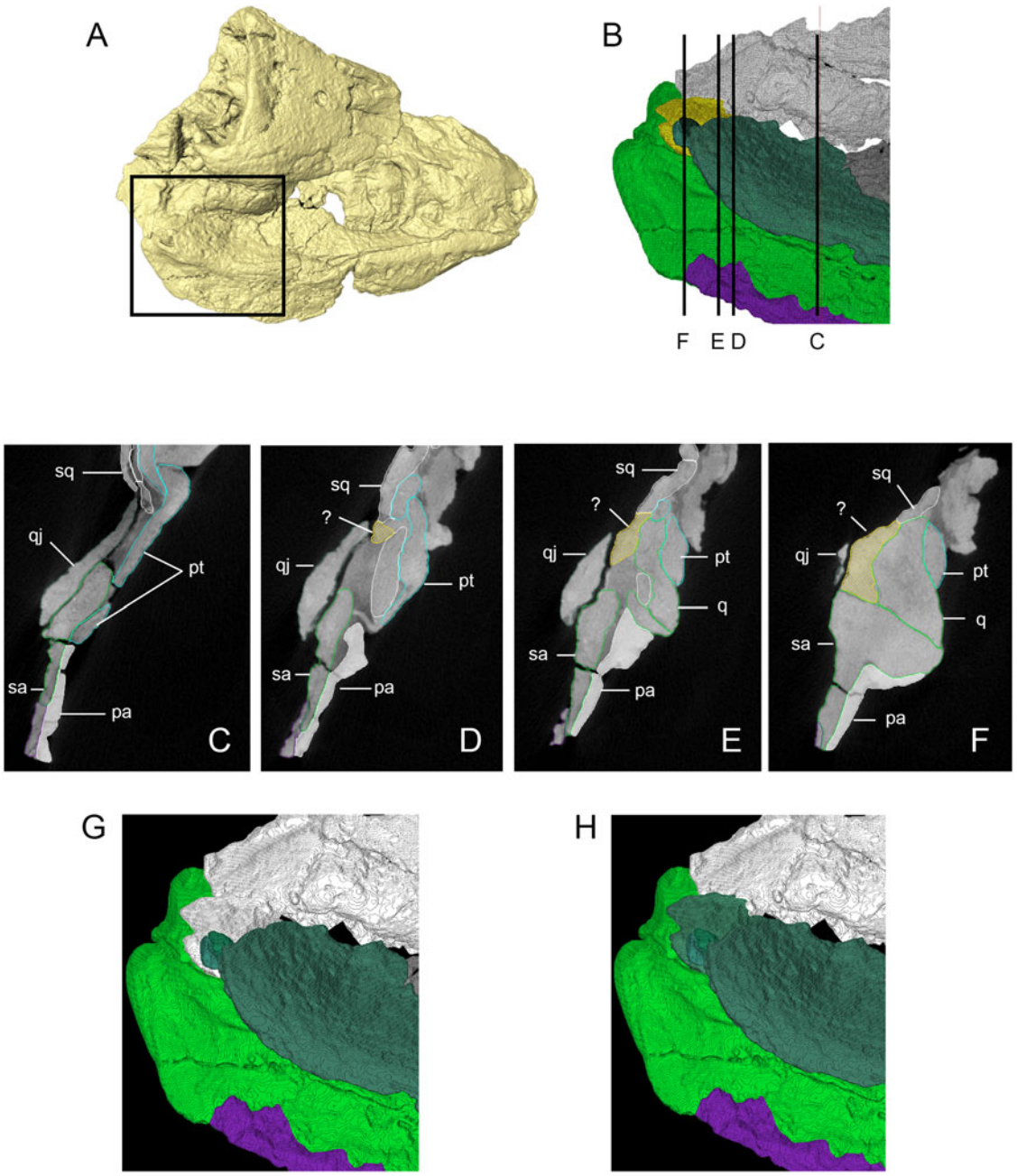

Figure 7 Three-dimensional (3D) isosurface, segmented model and transverse computed tomography (CT) slices from original scan data illustrating uncertain squamosal–quadrate–quadratojugal contact. (A) Dorsal/right lateral view of 3D isosurface of the skull with box delimiting area of (B). (B) Inset of (A) showing segmented model (individual bone colours the same as Figures 2 and 3, but with unknown fragment of bone shown in yellow), illustrating transverse sections shown in (C)–(F). (C)–(F) Transverse CT slices as shown in (B), unknown bone shown in yellow. (G) Segmented model showing unknown bone as fragment of the squamosal (following Panchen 1975). (D) Segmented model showing unknown bone as fragment of the quadratojugal (following Smithson 1985). Abbreviations: pa = prearticular; pt = pterygoid; q = quadrate; qj = quadratojugal; sa = surangular; sq = squamosal; ? = unknown fragment.

The quadratojugal (Figs 2, 3 and Supplementary Fig. 2) forms part of the ventral and posterior margins of the upper jaw; it is preserved nearly complete on the right side of the skull with only part of the anterior process preserved on the left. In transverse section, the quadratojugal was very gently laterally bowed with the ventral margin being mediolaterally wider than the dorsal margin. The ventral margin of the quadratojugal formed the lateral boundary of the subtemporal fossa. The medial aspect of the quadratojugal makes an extensive, sinuous contact with either the lateral surface of the squamosal or the quadrate, depending on the identity of the unknown piece of bone (see above).

The right quadrate of NMS G.1950.86 is preserved intact and in articulation with the lower jaw, with scans revealing numerous new details about this element (Figs 2, 3 and Supplementary Fig. 3). In lateral view, the quadrate is an irregular quadrilateral with straight posterior and ventral aspects, a nearly straight dorsal margin, and a sharp, anteroventrally sloping anterior margin. In anterior view, the quadrate is triangular in profile; in ventral view, it is tear-drop shaped, with a rounded posterolateral margin and a tapering anteromedial end. There is a single condyle, which is anteroposteriorly convex and mediolaterally concave; thus, it is saddle-shaped as in *Crassigyrinus* (Porro *et al*. 2023); however, the curvatures are far less pronounced and the joint surface more extensive and much flatter than in *Crassigyrinus*. The joint surface is ventrally directed and has sharply defined anterior and posterior margins. The anterolateral aspect of the quadrate dorsal to the joint surface is gently concave and relatively

https://doi.org/10.1017/S175569102300018X Published online by Cambridge University Press

small compared with the extensive, deeply excavated anterior surface of the quadrate in *Crassigyrinus* (Porro *et al*. 2023). The convex lateral surface broadly contacts the medial aspect of either the squamosal or quadratojugal (see earlier discussion). The medial aspect of the quadrate is concave, and in posterior view the quadrate appears to have dorsal and medial processes; the tapering posterior process of the pterygoid medially overlapped the convex dorsomedial aspect of the medial process of the quadrate.

2.2. Skull roof

Both nasals are present in NMS G.1950.86, although the right element is far more complete (Figs 2, 3 and Supplementary Fig. 4). In transverse section, it is gently dorsally arched and dorsoventrally thickest along its lateral margin, tapering medially. Its external surface is smooth and lacks the ridging seen in other taxa, such as *Crassigyrinus* (Porro *et al*. 2023). There is a notch in the anterior margin into which the tip of the premaxilla inserted. The anterior part of the lateral margin is gently embayed and formed the dorsal and medial margin of the external naris. The thickened lateral margin is concave, dorsally and laterally overlapping the dorsal margin of the lacrimal and the anterodorsal margin of the prefrontal. The anterior margin of the frontal dorsally overlaps the posterior margin of the nasal. The tapering medial margins of the nasals presumably met at the midline in a weak butt joint; however, this contact has been disrupted along the preserved lengths of the nasals. There is no conspicuous midline groove as in *Crassigyrinus* (Porro *et al*. 2023). The ventral (internal) surface of the nasal features a strong, rounded longitudinal ridge coursing from the anterior margin to approximately two-thirds the length of the element before it turns sharply laterally towards the articulation with the lacrimal. A second, more subtle longitudinal ridge branches from the sharp curve of the primary ridge and continues to the posterior margin of the nasal and onto the ventral surface of the frontal. The underside of the nasal lateral to the main ridge is strongly concave as clearly preserved on both sides of the specimen; this ridge may medially bound the laterally positioned nasal capsule (Rosen *et al*. 1981). Additionally, the ventral surface of the nasal between the two ridges is also depressed; this is continuous with and contributes to a circular depression across the internal surfaces of the nasal, frontal, prefrontal and lacrimal.

The right prefrontal (Figs 2, 3 and Supplementary Fig. 4) is well preserved and is triangular with its apex anteriorly directed and an embayed and thickened posterior margin that forms the anterior margin of the orbit. The lateral surface of the prefrontal anterior to the orbital ridge is weakly laterally bowed in transverse section and features a thickened ventral margin that laterally overlaps the dorsal margin of the lacrimal, as well as an inturned dorsal margin that is dorsally overlapped by the lateral margin of the frontal. Both Panchen (1975) and Smithson (1985) illustrate an uncertain contact between the anterior tip of the postfrontal and the posterior tip of the prefrontal. The left prefrontal is missing and the right postfrontal is missing its anterior margin; thus, this contact is not preserved in NMS G.1950.86. Our 3D reconstruction does not include a contact between the pre- and postfrontal. However, depending on the amount of the right postfrontal that is missing, contact between these elements may have been possible. The internal (medial) surface of the prefrontal between the inturned dorsal margin, thickened ventral margin and thickened orbital margin is strongly depressed, with this depression being continuous with that on the internal surface of the nasal.

The right frontal is mostly complete although the anterior end is missing its medial margin; only the posterior part of the left frontal is preserved (Figs 2, 3 and Supplementary Fig. 4). In transverse section, the anterior portion of the frontal is dorsoventrally tallest laterally and thins medially; the posterior portion is uniformly thick in cross-section. The ventral surface of the frontal features a longitudinal ridge continuous with the ridge on the underside of the nasal. This ridge terminates at the posterior corner of the frontal–prefrontal contact, and the ventral aspect of the frontal lateral to the ridge is concave, continuous with the depression on the internal surfaces of the nasal and prefrontal. The posterior half of the lateral edge of the frontal is gently embayed where it fits into a pronounced groove on the medial margin of the postfrontal with faint interdigitations visible. The posterior margin of the frontal meets the anterior margin of the parietal at a nearly vertical contact with interdigitations visible. The midline contact between the frontals has opened but appears to have been a weak butt joint. It is unclear whether the frontal contributed to the orbit as the uncertain contact between the prefrontal and postfrontal would exclude it from the orbital margin (see below).

The postfrontal is preserved on both sides of NMS G.1950.86, although the right element is missing its anterior tip (Figs 2, 3 and Supplementary Fig. 5). Anteriorly, the convex medial margin of the postfrontal is grooved and receives the lateral margin of the frontal in an interdigitated contact. The posteromedial margin of the postfrontal dorsally overlaps the lateral margin of the parietal in an interdigitating contact. The anterior tip of the left postfrontal of NMS G.1950.86 features a rounded facet that may represent the contact with the prefrontal, which is missing on the left side of the specimen; if so, this would have excluded the frontal from the orbital margin. We note this area of uncertainty in our interpretive drawings (Fig. 6) but do not attempt to reconstruct the potentially missing portion of the postfrontal in Figure 5. Our best approximation is that the prefrontal and postfrontal did contact at the orbital margin; however, we cannot be certain based on fossil evidence. The lateral margin of the postfrontal forms the upper border of the orbit; ventral and medial to this margin, the postfrontal features an elongate facet (that continues posteriorly onto the intertemporal), which presumably articulated with the postorbital, although this contact is not preserved. The posterior margin of the postfrontal meets the anterior edge of the intertemporal in an interdigitated contact.

The postorbital (Figs 2, 3) is only preserved on the right side of NMS G.1950.86 and is damaged and incomplete. In transverse section, it is mediolaterally widest at its ventral margin and thins dorsally. The ventral margin of the postorbital fits into a notch in the dorsal margin of the jugal. The posterior margin of the postorbital must have met the anterior margin of the squamosal at a dorsoventrally extensive contact; however, due to breakage of both the postorbital and the anterior margin of the squamosal, the morphology of this contact is unknown. Likewise, the contact between the postorbital and skull roof has opened but is almost certainly represented by the elongate depression on the ventrolateral margins of the posterior half of the postfrontal and anterior half of the intertemporal.

The parietal is complete on both sides of NMS G.1950.86 (Figs 2, 3 and Supplementary Fig. 5). In dorsal view it features straight anterior and medial margins, a convex lateral margin, an anteriorly concave posterior margin and a long, tapering posterolateral prong. There is a prominent, circular parietal foramen in the midline surrounded by a raised lip of bone on the dorsal aspect of the parietal; scans demonstrate that the foramen is situated in a deep circular depression encircled by a strong ridge on the ventral aspect of the parietals. In transverse section, the parietals form a flat skull table; their medial margins are thickest and the elements thin slightly laterally. The lateral margin of the parietal contacts the postfrontal, intertemporal and supratemporal. The medial margin of the intertemporal dorsally overlaps the lateral margin of the parietal in an interdigitated contact. The

https://doi.org/10.1017/S175569102300018X Published online by Cambridge University Press

contact between the supratemporal and parietal is more vertical and very tight; interdigitations may be present but are difficult to discern due to poor scan contrast and potentially partial fusion between the elements. The long, tapering posterolateral prong of the parietal wedges between the supratemporal (laterally) and tabular (medially); it meets the latter in a nearly vertical, interdigitated contact. The medial portion of the posterior margin of the parietal contacts the anterior margin of the postparietal in a vertical, interdigitating contact, and the two parietals contact each other at a sinuous midline suture with strong interdigitations.

The oval intertemporal forms part of the lateral margin of the skull roof between the postfrontal and supertemporal, being best preserved on the right side of NMS G.1950.86 with only a sliver of this bone preserved on the left (Figs 2, 3 and Supplementary Fig. 5). The posterior margin of the intertemporal dorsally overlaps the anterior margin of the supratemporal at an interdigitated suture. The anterior half of its lateral margin bears an elongate facet that continues anteriorly onto the postfrontal and presumably articulated with the postorbital. The posterior half of the lateral margin is rounded and roughened, with this margin continuing posteriorly onto the supratemporal. The lateral margins of both skull roof bones presumably fit against the gently grooved surface of the inturned dorsal margin of the squamosal.

In dorsal view, the supratemporal is mediolaterally narrower and anteroposteriorly more elongate than the intertemporal, being preserved on both sides of NMS G.1950.86 (Figs 2, 3 and Supplementary Fig. 5). In transverse section, the bone is mildly dorsally and laterally convex, and forms a folded edge to the posterior skull roof. The lateral margin of the supratemporal is rounded and roughened, and (with the exception of the posterolateral corner) presumably articulated with the flattened and gently grooved dorsal margin of the squamosal. The posterior part of the medial margin of the supratemporal meets the tabular in a vertical interdigitated contact, and there is no contact between the supratemporal and postparietal.

The tabular of *E. watsoni* (Figs 2, 3 and Supplementary Fig. 5) was extensively described by both Panchen (1975) and Smithson (1985), and there is little additional information to be added from scans of NMS G.1950.86. The right element is better preserved than the left side, with the latter missing most of the tabular horn. An anteromedial process of the tabular inserts between the posterolateral prong of the parietal and the postparietal, contacting both at tight, interdigitated, vertical sutures. The tubercle projecting from the ventral surface of the tabular horn described by Smithson (1985) is clearly visible on the right side, as is the ridge between this tubercle and the articular facet with the otic capsule. Smithson (1985) suggested that a roughened area on the ventral aspect of the tabular anterior to this tubercle may have contacted the quadrate wing of the pterygoid, either directly or via a ligament. The quadrate wing of the squamosal does not reach this roughened area in our 3D reconstruction, so any connection between the palate and tabular, if it existed, would have been via soft tissues. Viewed dorsally, the posteromedial margin of the tabular (medial to the horn) is smoothly and strongly embayed, terminating medially at a deep socket directed anteriorly, medially and ventrally, with pronounced raised edges that articulated with the otic capsules as described by Smithson (1985) in another specimen, NMS G.1975.48.48.

The postparietals form the gently embayed posterior margin of the upper jaw (Figs 2, 3 and Supplementary Fig. 5). In transverse section, the postparietals are dorsoventrally thickest at their medial margins, where they contact each other at a nearly fused vertical suture, and thin slightly laterally. Laterally, the posterior surface of the postparietal bears a concavity continuous with the embayed posteromedial surface of the tabular and dorsally bordered by a ridge; medially, there is a midline projection ventral to the ridge. Panchen (1975) labelled a bony mass posterior to these projections in NMS G.1950.86 as the supraoccipital, whereas Smithson (1985) identified this mass as part of the axis. This bony mass was impossible to segment from the surrounding matrix in our scans and we have no further insight into its identity. The posteroventral margins of the postparietals are smoothly rounded; they presumably articulated with the otic capsules (Smithson 1985) but there are no clear facets for this contact visible in our scans.

2.3. Palate

CT scans shed new light on the previously undescribed vomer of *E. watsoni* (Figs 2, 3 and Supplementary Fig. 6). The left vomer appears to be largely intact but deformed. As preserved, the vomer is anteroposteriorly elongate and mediolaterally narrow; it is transversely widest at its anterior and posterior ends, and constricted in its centre, probably as a result of forming the medial boundary of the choana. Scans demonstrate the vomer is nearly round in transverse section anteriorly. Posteriorly, it flattens dorsoventrally and bears the posterior teeth (see below) on a thickened ventral ridge that supports an expanded lateral process and a shorter dorsomedially directed process; thus, it is an asymmetric V-shape in transverse section. Scans reveal the presence of seven teeth in the vomer. The first tooth is of medium size and is followed by three large vomerine fangs, with only the stump of the first fang preserved and the second and third fangs having been broken at their bases and folded over medially and posteriorly. Nonetheless, the third fang is the best preserved and appears to have been nearly straight in mediolateral view and very gently curved medially in anterior view. The fangs are followed by three small posterior teeth on the ventral ridge of the vomer. The rounded anterior margin of the vomer laterally contacts the medial aspect of the premaxilla (although given that much of the left premaxilla is missing, it is likely that this contact was originally more extensive). Presumably, the vomer met its counterpart across the midline anteriorly and medially, although there is no trace of the right vomer. At the midpoint of the element, the lateral margin is embayed and forms the medial wall of the choana. The ragged posterior margin of the vomer would have fit against the anterior margin of the palatine, although this contact has opened on the left (and the left palatine has been rotated nearly 180 degrees on its long axis by deformation) and the right vomer is missing. The elongate anterior process of the pterygoid fit against the curved medial border of the vomer, with the short dorsomedial process of the vomer dorsally overlapping the anterior process of the pterygoid.

The palatine is preserved on both sides of NMS G.1950.86 (Figs 2, 3 and Supplementary Fig. 6), although as previously noted the left palatine has been rotated nearly 180 degrees about its long axis by deformation. It is mediolaterally widest at its anterior end and narrows posteriorly. The anterior margin is strongly embayed to form the posterior wall of the internal choana with a short and pointed anterolateral process – which formed part of the lateral wall of the choana and contacted the maxilla – and a larger anteromedial process with a scalloped anterior margin that met the posterior margin of the vomer. In transverse section, the palatine is dorsoventrally tallest laterally and tapers medially to form a thin, extensive shelf. The lateral margin is dorsoventrally expanded and concave along its entire length, where it articulated with the medial shelf of the maxilla and, potentially, the ventromedial edges of the lacrimal and anterior jugal. In dorsal view, the junction between the concave lateral margin of the palatine and the relatively flat dorsal aspect of the extensive medial shelf results in a rounded longitudinal ridge that courses along the entire length of the element. The

https://doi.org/10.1017/S175569102300018X Published online by Cambridge University Press

right palatine preserves the stumps of two large fangs and a large replacement pit immediately posterior to the margin of the choana, as described by Panchen (1975). In contrast, the left palatine bears the stumps of two large fangs anteriorly, followed by the remains of five smaller teeth posteriorly. The medial shelf of the palatine is extensively underlapped by the lateral margin of the pterygoid and the posterior end of the palatine is underlapped by the anterior margin of the ectopterygoid.

The posterior margin of the internal choana is well defined and formed by the palatine. Its medial margin, formed by the vomer, is more uncertain, and its lateral margin is inferred to have been formed by the maxilla. As previously noted, it is unclear whether the premaxilla contributed to the margin of the choana due to the missing posterior end of the element. Despite these uncertainties, the internal choana is positioned ventral and only slightly posterior to the external naris in our reconstruction (Fig. 3C).

The ectopterygoid is anteroposteriorly elongate and mediolaterally narrow (Figs 2, 3 and Supplementary Fig. 7). The right ectopterygoid of NMS G.1950.86 appears to be complete although broken at its midpoint whereas only the anterior half of the left element is preserved. It is nearly square in transverse section, with a concave lateral surface that articulated with the maxilla and a subtle medial shelf underlapped by the lateral margin of the pterygoid. It is possible that the ventromedial margin of the jugal contacted the dorsolateral edge of the ectopterygoid, but this cannot be confirmed. The rounded anterior margin underlapped the posterior end of the palatine and the posterior end of the ectopterygoid formed the anterior margin of the subtemporal fossa. The right ectopterygoid contains nine teeth: two smaller teeth anteriorly, the stumps of two enlarged ectopterygoid fangs and five small teeth posterior to the fangs. The incomplete left ectopterygoid contains seven teeth: two enlarged fangs followed by five smaller teeth. The second fang on the left side is the only well-preserved ectopterygoid fang, being nearly vertical in lateral view and slightly medially curved in anterior view.

The pterygoid is the largest bone of the palate and is composed of an anterior process, the horizontal main body, and a vertical quadrate ramus (Figs 2, 3, 5, 8 and Supplementary Fig. 7). The main body and anterior process of the right pterygoid are largely complete except in the region of the basal articulation. Scans reveal that the right quadrate ramus has been broken by deformation, folded over the basisphenoid, and is hidden under overlying layers of bone. The left pterygoid has been broken into numerous pieces, with one of the largest fragments preserving the basal articulation. The pterygoid is mediolaterally widest at the level of the pterygoid flange. Anterior to the ectopterygoid–palatine contact, the pterygoid tapers medially to a blunt point, forming the anterior process, which underlapped the medial margin of the vomer and extensively underlapped the medial shelf of the palatine. The anterior process of the pterygoid is relatively thick dorsoventrally in transverse section; moving posteriorly, the main body expands laterally, thins dorsoventrally and becomes gently dorsally arched in cross-section. The medial margin thickens dorsoventrally approaching the basal articulation; the main body thins laterally and underlaps the short medial shelf of the ectopterygoid. The medial margins of the anterior processes of the pterygoids presumably contacted each other at the midline; however, no part of this contact is preserved.

Posteriorly, the parasphenoid inserts between the pterygoids, and scans demonstrate that the thickened medial margin of the pterygoid contacted the lateral aspect of the parasphenoid in a vertical butt joint. The concave socket that articulated with the basipterygoid process is mediolaterally expanded so that it is approximately three times as wide as it is dorsoventrally tall. It faces posteriorly and medially, and is surrounded by a raised lip of bone. Anterior to the level of the basal articulation, the pterygoid and ectopterygoid separate and the pterygoid forms the medial margin of the subtemporal fossa. However, unlike other early tetrapods such as *Acanthostega* (Porro *et al.* 2015b), *Crassigyrinus* (Porro *et al.* 2023) and *Whatcheeria* (Rawson *et al.* 2021), the pterygoid of *E. watsoni* does not immediately narrow at this point but instead expands laterally to form a gently rounded, ventrolaterally directed pterygoid flange (Fig. 8). Posterior to the flange, the horizontal lamina of the pterygoid abruptly narrows medially and terminates at a rounded point that overlapped the medial aspect of the quadrate. The quadrate ramus of the right pterygoid was originally a sheet of bone rising from the medial margin of the horizontal main body. The anterior margin of the quadrate ramus is broken and missing. As preserved, it is dorsoventrally tallest at the level of the pterygoid flange and its posterior border slopes down to join the tapering posterior process of the main body. The dorsal margin of the quadrate ramus presumably met the dorsomedial margin of the squamosal, although this contact is not preserved.

2.4. Braincase

The identification and morphology of various elements of the braincase of NMS G.1950.86 are a point of disagreement between descriptions by Panchen (1975) and Smithson (1985). Panchen (1975) did not identify many braincase elements in his line drawings of the skull but did provide verbal descriptions of their locations. Smithson (1985) used the better-preserved occiput of NMS G.1975.48.48 to reinterpret many features in the type and provided clearly labelled interpretive line drawings.

The basisphenoid and parasphenoid are visible in ventral view (Figs 2, 3 and Supplementary Fig. 8). As noted by Smithson (1985), these elements are indistinguishably fused, although there is a break anterior to the base of the cultriform process of NMS G.1950.86. The cultriform process of the parasphenoid is mediolaterally widest and dorsoventrally tallest at its base and tapers anteriorly, inserting between the pterygoids and contacting the medial margins of the pterygoids at vertical butt joints. Scans reveal that the dorsal surface of the parasphenoid features a shallow, U-shaped groove. Posteriorly, this groove deepens and terminates as a deep, anteriorly-facing pit bounded dorsally by a midline vertical projection of bone. This pit is too far anterior to be the retractor pit or sella turcica (see below) and its identity is unclear, but it may represent the course of the internal carotids or tracts of the optic chiasma. As preserved the parasphenoid reaches the level of the midpoint of the ectopterygoid, although it may have extended as far anteriorly as the ectopterygoid–palatine process based on the curved shape of the medial margin of the right pterygoid. As noted by both Panchen (1975) and Smithson (1985), the ventral aspect of the parasphenoid is ornamented, with a longitudinal midline ridge and the lateral surfaces of the base of the cultriform process, immediately anterior to the basipterygoid processes, being shallowly excavated to accommodate the sockets of the basal articulation of the pterygoid.

In ventral view, the basisphenoid is triangular with its apex directed anteriorly, and is mediolaterally expanded posterior to the basal articulation. As noted by Smithson (1985), Panchen (1975) misinterpreted the midline of the basisphenoid in NMS G.1950.86 and reconstructed the bone with a triradiate posterior border, supporting a close relationship with seymouriamorphs. Our scans support Smithson's (1985) interpretation: a V-shaped posterior margin bounded by pointed flanges of bone that presumably clasped the basioccipital in life. Medial to the basipterygoid processes, there are two short longitudinal ridges bounding a midline groove as well as lateral grooves between these ridges and basipterygoid processes that mark the course of the internal carotid arteries (Smithson 1985). These ridges and grooves

https://doi.org/10.1017/S175569102300018X Published online by Cambridge University Press

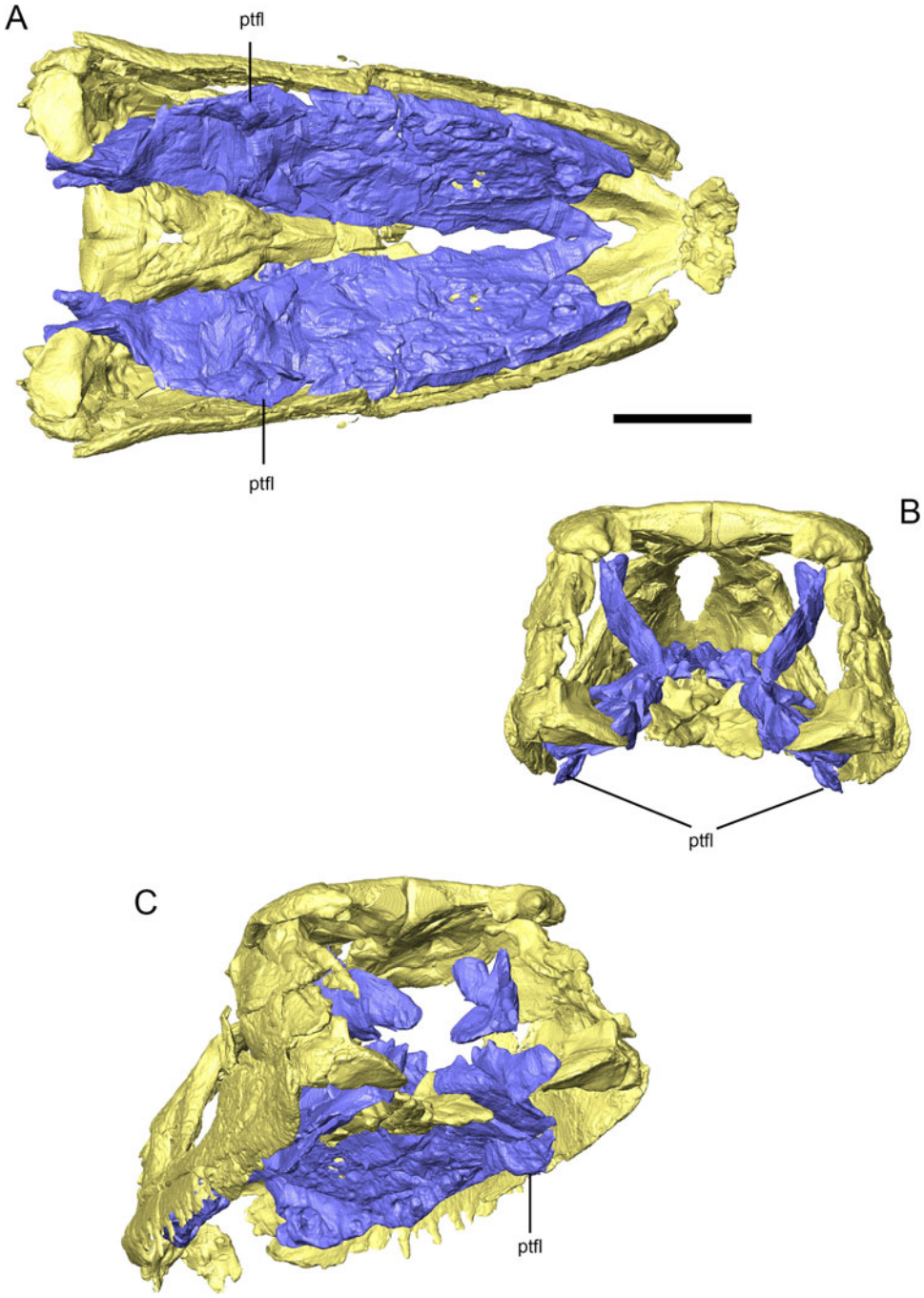

Figure 8 Three-dimensional reconstruction of the skull of *Eoherpeton watsoni* highlighting the pterygoid and pterygoid flange (purple) compared with the rest of the upper jaw (yellow). (A) Ventral view of the upper jaw and pterygoid. (B) Posterior view of the upper jaw and pterygoid. (C) Posteroventral oblique view of the upper jaw and pterygoid. Abbreviations: ptfl = pterygoid flange. Scale bar = 30 mm; no scale bar for oblique view.

flatten posteriorly and the ventral aspect of the posterior basisphenoid is unornamented.

Smithson (1985) provided a detailed description of the basipterygoid process of *E. watsoni* based on NMS G.1975.48.48. Scans reveal more details of the processes in NMS G.1950.86. The processes project laterally, anteriorly and very slightly ventrally. They are mediolaterally expanded to a greater degree than they are dorsoventrally expanded, matching the proportions of the corresponding socket on the pterygoid. There is a single, relatively flat articular surface preserved in NMS G.1950.86 unlike the two distinct articular surfaces described by Smithson (1985) in NMS G.1975.48.48; however, this could be due to poorer preservation of these surfaces in the type, limits of scan resolution or both. Both sides feature defined anterior, ventral and posterior margins; the process on the right also has a defined dorsal margin, whereas the dorsal aspect of the left process grades smoothly onto the lateral aspect of the basisphenoid; this may be an artefact of erosion.

In lateral view, there are pronounced projections rising from the lateral margins of the basisphenoid immediately posterior to the level of the basipterygoid processes, identified by Smithson (1985) and by ourselves as the dorsum sellae although they may grade into the pila antoticae as described in the lysorophian *Brachydectes* (Pardo & Anderson 2016); however, no contact between these processes and the parietals are preserved in this specimen. There is a circular depression between and anterior to these lateral walls and posterior to the midline projection of bone at the base of the cultriform process. This depression marks the origin of the retractor bulbi muscles (retractor pit), as identified by Smithson (1985) in *E. watsoni* and in the same

https://doi.org/10.1017/S175569102300018X Published online by Cambridge University Press

position dorsal to the basipterygoid processes in other embolomeres (Clack & Holmes 1988). The posterior portion of this depression may represent the hypophyseal fossa/sella turcica, which is always located posterior to the retractor pit (Clack & Holmes 1988) but there is no evidence to delineate precise boundaries between these structures. Both aforementioned lateral projections feature smoothly excavated posterior surfaces that formed the anteroventral margin of the fenestra ovalis (Smithson 1985). Posterior to the lateral projections, the dorsal margin of the basisphenoid is initially ventrally concave (forming the ventral margin of the fenestra ovalis), then rises as a rounded flange before tapering to posterior tip of the basisphenoid. In dorsal view, the dorsal aspect of the basisphenoid posterior to the lateral projections is a wide, shallow U-shaped depression that floored the braincase and presumably underlapped the basioccipital.

The fragment of epipterygoid described (but not figured) by Panchen (1975) cannot be discerned, and it may be possible that the poorly preserved basal articulation of the right pterygoid was mistaken for the conical recess of the epipterygoid.

Panchen (1975) stated that the supraoccipital, opisthotic and right exoccipital were visible in dorsal view, and that the basioccipital was located immediately ventral to the right tabular horn. Smithson (1985) reinterpreted the mass identified by Panchen (1975) as the right exoccipital as the axis, and our scans demonstrate that the bone identified by Panchen (1975) as the basisphenoid is instead part of the right exoccipital (see section below on the exoccipital). The supraoccipital and otic capsules identified by Panchen (1975) cannot be distinguished from surrounding bone and matrix because of poor contrast and, therefore, could not be segmented, so no further useful anatomical information could be obtained on these elements.

Smithson (1985) reinterpreted various structures on the ventral aspect of the skull as portions of the braincase, including the right exoccipital, which was originally identified by Panchen (1975) as part of the basisphenoid (Figs 2, 3 and Supplementary Fig. 8). Part of this bone is also exposed in dorsal view of the occiput. Scans provide new visualisations of this element, but its morphology is difficult to interpret. In ventral view (with reference to the entire specimen, not the isolated bone), the element has a rectangular base that abruptly narrows to a short, rounded tip. The posteriorly directed margin features a pronounced oval facet surrounded by a sharp rim of bone. The anteriorly directed margin, in contrast, is smoothly convex. In dorsal view (with reference to the entire specimen), the element features a strong, rounded ridge from the rounded tip to the base, with the surfaces on either side of the ridge being strongly depressed.

Smithson (1985) also identified a fragment of the basioccipital visible in ventral view. Although this element was segmented out, data from scans do not provide any useful additional data on this element.

Panchen (1975) and Smithson (1985) produced very different reconstructions of the occiput in *E. watsoni*, in particular regarding the orientation of the exoccipital and its contacts with surrounding bones. Our scan data more strongly supports Smithson's (1985) interpretations of various braincase elements in *E. watsoni*. However, with the exception of the basisphenoid and parasphenoid, insufficient scan contrast prevented clean segmentations of many of the braincase elements – particularly the otic capsules – and for this reason we do not attempt a reconstruction of the occiput of this taxon in the present work.

2.5. Lower jaw

The lower jaw of *E. watsoni* was described by Panchen (1975) with additional data presented by Smithson (1985). The right ramus of NMS G.1950.86 is better preserved than the left, although the postdentary portion has been mediolaterally compressed, the anterior third of the lower jaw has been deformed (with the dorsal margin twisted laterally about the anteroposterior axis), and there is a substantial break across the middle of the ramus. The left ramus has experienced greater erosion, its posteroventral portion is missing, and many of the postdentary bones have been broken and compressed. The postdentary region of the jaw is dorsoventrally expanded, although this may be somewhat exaggerated by deformation, whereas the tooth-bearing region of the jaw is dorsoventrally thinner with the dorsal and ventral margins nearly parallel. Compared with earlier tetrapods, such as *Acanthostega* (Porro *et al.* 2015b), *Brittagnathus* (Ahlberg & Clack 2020) and *Crassigyrinus* (Porro *et al.* 2023), the anterior lower jaw of *E. watsoni* is relatively straight in lateral view, with the posteroventral margin curving towards the jaw joint and the dorsal margin of the postdentary region exhibiting a pronounced surangular crest, the point at which the jaw is dorsoventrally tallest. Scans demonstrate that the surangular crest is distinctly angled in lateral view as described by Smithson (1985), not gently rounded as illustrated by Panchen (1975). The ventromedial margin of the splenial and ventral margin of the postsplenial are drawn into a well-defined ridge, although there is no ventral keel running the entire length of the lower jaw as in *Crassigyrinus* (Porro *et al.* 2023). The lateral aspect of the lower jaw is made up of the dentary and four infradentary bones, whereas the medial aspect is made up of the medial laminae of the splenial, postsplenial and angular, the prearticular and the coronoids. There is no single large Meckelian fenestra but instead a series of small openings between the prearticular and medial laminae of the postsplenial and angular. In dorsal view, the lower jaw is relatively straight with the front of the ramus curving medially to meet its counterpart at the symphysis. The mandibular adductor fossa occupies the posterior third of the lower jaw.

The dentary (Figs 2, 4 and Supplementary Fig. 9) is dorsoventrally tallest at about one-third of its length from its posterior end, tapering gently towards its rounded anterior end and much more abruptly towards its posterior end, which terminates as a pointed spike overlying the surangular. In dorsal view, the dentary is narrowest at its posterior end and widens gradually towards the symphysis. The anterior two-thirds of the dentary is rounded in transverse section, with the posterior third being laterally bowed with a thickened dorsal margin supporting the teeth, a ventral lamina that contacts the postsplenial and angular, and a medial shelf that contacts the posterior coronoid. Although there are small canals leading to pores on the surface, the anterior end of the dentary is solid bone and the Meckelian canal (enclosed by the dentary and splenial) ends at the level of the third or fourth dentary tooth; it does not open into the symphysis as in earlier tetrapods (Porro *et al.* 2015a, 2015b). There are few intact dentary teeth, although scans can give an idea of tooth count. The right dentary contains 25 teeth, more than that illustrated by either Panchen (1975) or Smithson (1985). Compared with other early tetrapods, the dentary teeth of *E. watsoni* are remarkably uniform in size. The first eight teeth appear to be relatively uniform in size (but see below); these are followed by eight more teeth that are slightly smaller, then a slightly enlarged 17th tooth and the final eight teeth that are similar in size to the anterior eight. The third and fifth right dentary teeth are well preserved enough to give an idea of tooth shape, although both have been displaced. They suggest the teeth were posteriorly recurved and sharply pointed. Remnants of the first tooth suggest it was similar in size to immediately succeeding teeth; however, it is set within a particularly deep pit with well-defined bony margins that project above the dorsal margin of the dentary. Thus, it is possible the most anterior tooth was originally much larger, and perhaps even a dentary tusk. Due to poor contrast between the left dentary teeth and

https://doi.org/10.1017/S175569102300018X Published online by Cambridge University Press

surrounding bones and matrix, only three left dentary teeth could be segmented from our data although it is certain that more are preserved within the dentary.

In medial view, there is a crescentic surface on the medial aspect of the anterior surface of the dentary that continues onto the splenial, most likely representing its contact with its counterpart across the symphysis. The size of the contact area suggests a relatively restricted butt contact between the left and right dentaries and splenials. The ventrolateral edge of the dentary meets the dorsolateral margin of the splenial in a curved butt contact. In most early tetrapods, the ventral margin of the dentary laterally overlaps the infradentary bones. In *E. watsoni*, the ventral margin of the dentary laterally overlaps the angular, tapering posteriorly to a point laterally overlying the surangular; unusually, however, the dorsolateral margin of the postsplenial laterally overlaps the ventral margin of the dentary. The long anterior process of the angular inserts medial to the dentary and extensively contacts its medial surface. As noted below, contrast between the coronoids and adjacent bones (and each other) is poor, and it is sometimes impossible to visualise their boundaries. The lateral aspect of the right anterior coronoid contacts the medial aspect of the dentary below the level of the tooth bases; faint interdigitations may be present but cannot be confirmed. The boundary between the dentary and coronoid series is lost between the level of the 12th and 16th dentary teeth; when the dentary-coronoid boundary clearly reappears in scans, the coronoids are sutured to the medial shelf of the dentary, with their dorsal margins level with the alveolar margin of the dentary and faint interdigitations visible. Scans demonstrate point contacts between the dorsal margins of the prearticular and the dentary, but these are almost certainly artefacts of deformation.

The splenial (i.e., presplenial of Smithson [1985]) is anteroposteriorly elongate and dorsoventrally narrow, and forms the anteroventral margin of the lower jaw (Figs 2, 4 and Supplementary Fig. 9). It is V-shaped in transverse section, although the lateral lamina – which contacts the dentary and postsplenial – is very short compared with the longer medial lamina. Anteriorly, the medial aspect of the medial lamina – which contacts the dentary and coronoid series – is slightly depressed; posteriorly, it becomes medially convex. The apex of the V that joins the two laminae in cross-section forms the sharp ventral margin of the lower jaw. The anterior margin of the splenial is squared off and the crescentic symphysial surface of the dentary continues a short way onto the splenial, implying it also contacted its counterpart at the midline in a loose butt contact. There is a short, rounded anterodorsal prong near the anterior margin of the splenial that medially overlapped a corresponding short projection of the dorsomedial surface of the dentary. The anterior process of the postsplenial wedges between the dentary and splenial; posteriorly, the posterior process of the splenial ventrally underlaps the postsplenial, the two bones sharing an extensive contact. Posteriorly, the dorsal margin of the medial lamina contacts the ventral margin of the anterior coronoid, although the nature of this contact cannot be discerned in scans. The anterior tip of the prearticular does not reach the splenial in NMS G.1950.86 as depicted by Panchen (1975) and unlike the reconstruction by Smithson (1985); the posterior process of the splenial could not be seen overlapping the prearticular as described (but not figured) by Ahlberg & Clack (1998).

The postsplenial is an anteroposteriorly elongated bone (Figs 2, 4 and Supplementary Fig. 10). In transverse section, its anterior end is mediolaterally expanded and blade-shaped where it inserts between the dentary and splenial; there is a distinct overlap surface for the splenial on the anteroventral aspect of both the right and left postsplenials of NMS G.1950.86. In its middle and posterior portions, the postsplenial is U-shaped in transverse section, forming the floor of the Meckelian canal and the rounded ridge defining the ventral margin of the mandible. Its lateral wall laterally overlaps the ventral margin of the dentary while the medial wall contacts the ventral margin of the prearticular, although this suture has been disrupted throughout its length. Both Panchen (1975) and Smithson (1985) reconstructed the postsplenial–prearticular (and angular–prearticular) contacts in the typical morphology of embolomeres, forming a series of small openings rather than an enlarged Meckelian fenestra. The tapering posterior tip of the postsplenial ventrally underlaps the angular, and the long anterior process of the angular inserts dorsal to the postsplenial.

The angular (Figs 2, 4 and Supplementary Fig. 10) is a sickle-shaped bone that forms the posteroventral margin of the lower jaw and is tallest at its midsection, tapering anteriorly and posteriorly. In transverse section, it is mediolaterally widest near its ventral margin, tapering dorsally. Its dorsal margin is laterally overlapped by the dentary and the anterior part of the surangular; however, posteriorly the direction of overlap reverses and the dorsal margin of the angular laterally overlaps the ventral margin of the surangular. Scans reveal an elongate anterior process of the right angular of NMS G.1950.86 that inserts medial to the dentary and dorsal to the postsplenial, tapering to a point at the level of the 16th dentary tooth, forming the lateral wall of the Meckelian canal. The right angular of NMS G.1950.86 also preserves a medial lamina that rises from the ventral margin of the angular and medially overlaps the ventral margin of the prearticular.

The contact between the surangular and articular could not be resolved in CT scans (Figs 2, 4 and Supplementary Fig. 11), and it seems likely that the two bones have fused, as suggested by Panchen (1975). The surangular forms the posterolateral part of the lower jaw and its posterior margin. It is roughly pentagonal in lateral view with a straight, posterodorsally inclined posterior border and a slightly concave dorsal border leading to a sharply angled surangular crest, as reconstructed by Smithson (1985). Anterior to the crest, the straight anterodorsal edge and squared-off anterior margin of the surangular contact the coronoid, dentary and angular. The ventral margin of the surangular contacts the angular in an overlapping suture, previously described. The surangular forms most of the lateral wall of the mandibular adductor fossa. In transverse section, its dorsal margin is thickened and the bone tapers ventrally. As described by Smithson (1985), the lateral surface of the surangular posterior to the tip of the dentary features a longitudinal horizontal shelf; unlike in NUZ 78.1.61 (where NUZ is the institutional abbreviation for Department of Zoology, University of Newcastle Upon Tyne, United Kingdom) described by Smithson (1985), in NMS G.1950.86 this shelf continues to and merges with the lateral lip of the glenoid. The shelf divides the lateral aspect of the surangular into two faces: a convex dorsolaterally-facing aspect dorsal to the shelf and a concave, heavily ornamented ventrolaterally-facing aspect ventral to the shelf. Anterior to the surangular crest, NMS G.1950.86 preserves an anteriorly tapering sliver of bone. Panchen (1975) reconstructed this area as part of the surangular whereas Smithson (1985) identified this area as part of the posterior coronoid based on information from another specimen. Based on information from scans, we identify this sliver of bone as the posterior end of the posterior coronoid; however, there is some uncertainty in this identification. The ventral margin of this piece of posterior coronoid contacts the anterior margin of the base of the surangular crest in a butt joint. Ventral to this contact, the tapering posterior point of the dentary laterally and dorsally overlies the anterodorsal margin of the surangular.

Posteriorly, the surangular wraps around and forms the posterior margin of the lower jaw (Figs 2, 4 and Supplementary

https://doi.org/10.1017/S175569102300018X Published online by Cambridge University Press

Fig. 11). Data from scans of NMS G.1950.86 support Panchen's (1975) reconstruction of the lower jaw rather than Smithson's (1985) reconstruction, in which the angular forms much of the posterior border of the mandible; however, it should be noted that the latter was based on another specimen, NUZ 78.1.61. The posterior end of the prearticular medially overlaps the medial aspect of the surangular/articular in an extensive interdigitated suture. Lateral to the glenoid, the surangular thickens to form a pronounced lip, ventral to which is a triangular depression on the lateral surface with its apex directed posterodorsally. The posterior margin of the lower jaw, formed by the surangular, is also a thickened column of bone that continues dorsally to form a rounded, short dorsal tubercle (i.e., retroarticular process of Panchen [1975]). There are raised edges of bone defining both the anterior and posterior boundaries of the glenoid. Medially, the surangular/articular features a sharp, nearly vertical buttress continuous with the pronounced medial edge bordering the glenoid. Between this buttress and the posterior edge of the mandible, the medial surface is again strongly depressed. Panchen (1975) suggested the depressions on both aspects of the surangular ventral to the glenoid served as areas of muscle attachment.

As noted previously, the articular cannot be separated from the surangular in scans, possibly as a result of fusion between these bones, and it is possible that the surangular contributes to the joint surface (Figs 2, 4 and Supplementary Fig. 11). In dorsal view, the joint surface is kidney-shaped and is anteromedially inclined. As previously described, it is completely surrounded and delineated by raised edges of bone. The joint surface is anteroposteriorly concave and mediolaterally convex, matching the corresponding surface of the quadrate. A subtle midline ridge separates the joint into two faces, as described by Smithson (1985) in NUZ 78.1.61. Below the anterior edge, the anterior aspect of the articular/surangular is deeply concave and forms the posterior wall of the mandibular adductor fossa. This joint morphology, visualised for the first time in NMS G.1950.86 using CT scans, is nearly identical to that described by Smithson (1985) in NUZ 78.1.61.

The coronoid series (Figs 2, 4) forms the dorsal margin of the anterior part of the lower jaw in medial view; however, because of poor contrast between the coronoids and surrounding bones, some of the contacts are uncertain. Scans support the presence of a tapering anterior process of the prearticular that wedges between the anterior coronoid (dorsally) and the postsplenial (ventrally), thus supporting the reconstruction by Smithson (1985) rather than that by Panchen (1975) in which this anterior piece of bone was incorrectly identified as the anterior coronoid. Instead, scans demonstrate an anteroposteriorly elongated and dorsoventrally narrow strip of bone applied to the medial surface of the dentary below the level of the tooth bases. It can be discerned as far anteriorly as the fifth dentary tooth and posteriorly to the level of the 12th dentary tooth. It is mediolaterally narrow in transverse section and its ventral margin contacts the splenial; there is no contact between the anterior coronoid and postsplenial, as described by Panchen (1975). No teeth can be clearly discerned on the anterior coronoid. The coronoids cannot be discerned between the level of the 12th and 16th dentary teeth. When the coronoids are distinct again, the dorsal margin is level with the alveolar margin of the dentary. The contact with the dentary is tight but nothing more can be discerned of sutural morphology between these elements. The ventral margins of the middle and posterior coronoids contact the thickened dorsal edge of the prearticular; it is unclear whether the prearticular also contacted the anterior coronoid as the contact between the anterior and middle coronoids cannot be resolved. The contact between the middle and posterior coronoids cannot be discerned in CT slices, but from surface renderings, the junction between these elements appears to be approximately at the level of the 22nd dentary tooth, which would be further anterior than either Panchen (1975) or Smithson (1985) placed this contact. Surface renderings also clearly show the presence of three small coronoid teeth, approximately at the level between the 16th and 17th dentary teeth, presumably on the middle coronoid. As noted previously, we identify a sliver of bone that reaches the base of the surangular crest as the posterior coronoid, but this identification is uncertain.

The prearticular of *E. watsoni* is sickle-shaped, with a relatively straight posterior border, ventrally curved dorsal and ventral margins, and a tapering, pointed anterior process (Figs 2, 4 and Supplementary Fig. 10). It forms the posteromedial aspect of the lower jaw, the medial wall of the mandibular adductor fossa and the dorsal margins of the small Meckelian openings. In transverse section, it is a mediolaterally thin sheet of bone. Posteriorly, the dorsal margin is thickened and the bone thins ventrally; anteriorly, the bone is more a uniform thickness through its height. The ventral margin of the prearticular passes medial to the medial lamina of the angular and makes curved butt contacts with the margins of the angular and postsplenial. The dorsal margin contacts the ventral margins of the posterior and middle coronoids; as previously noted, it is uncertain whether the prearticular reached the anterior coronoid. The tapering anterior process of the prearticular is applied to the internal surface of the dentary, although this is probably an artefact of deformation.

3. Three-dimensional reconstruction of the skull of *Eoherpeton watsoni*

There have been two principal reconstruction attempts of the skull of *E. watsoni*. Panchen (1975) restored the skull with a classic reptilomorph shape – compared to earlier tetrapods, the skull of *E. watsoni* is relatively tall dorsoventrally, the snout and anterior skull roof are gently rounded in lateral view, and the skull table is nearly horizontal. The orbit is square-shaped and the posterior margin of the upper jaw nearly vertical, in contrast to the sloping, rounded posterior skull margins of earlier tetrapods (Porro *et al*. 2015b, 2023). In dorsal view, the skull is relatively narrow mediolaterally with a rounded snout that widens gradually posteriorly towards the jaw joints. The interorbital region of the skull roof is relatively wide and the orbits are laterally directed in contrast to the dorsolaterally directed orbits of earlier forms. In ventral view, the subtemporal fenestrae have a sinuous outline. In posterior view, the sidewalls of the skull are nearly vertical and the pterygoid flange projects below the ventral margins of the facial bones.

A later reconstruction by Smithson (1985) based on information from additional specimens differed from that of Panchen (1985) in several aspects. In lateral view, the premaxilla is reoriented and anteroposteriorly extended, the squamosal does not extend posteriorly behind the quadratojugal, and there is a sharper angle between the squamosal, supratemporal and tabular. In dorsal and ventral views, the reconstruction by Smithson (1985) is relatively wider than that by Panchen (1975) with a more rounded snout and mediolaterally wider vomers and palatines. This is likely because Smithson (1985) reconstructed the sidewalls of the skull as more laterally inclined in posterior view. The ventral edge of the pterygoid flange is level with the ventral margins of the facial skeleton rather than projecting below them. Additionally, the posterior surface of the quadrate is exposed in Smithson's (1985) reconstruction.

Reconstructions of the lateral aspect of the lower jaw are similar between the two authors, although the lower jaw is straighter (in lateral view) in Smithson's (1985) version and the surangular–angular contact at the posterior margin of the lower jaw is more

https://doi.org/10.1017/S175569102300018X Published online by Cambridge University Press

dorsally positioned. In medial view, the contact between the prearticular and surangular/articular is more anteriorly placed in Panchen's (1975) reconstruction than in Smithson's (1975), but the principal difference between the two reconstructions of the lower jaw is the arrangement of the coronoid series. Panchen (1975) reconstructs the anterior coronoid in a ventral and posterior position, contacting the postsplenial and preventing contact between the splenial and prearticular. In contrast, Smithson (1985) reconstructed an elongate anterior coronoid ventral to the tooth row stretching nearly to the symphysis, separated from the postsplenial by the anterior process of the prearticular, and with a splenial–prearticular contact.

Our 3D reconstruction (Figs 3–6), based on µCT data, features a skull roof that – in lateral view – slopes smoothly from the posterior end of the skull to the front of the snout, without the distinct change in slope anterior to the orbit featured in both previous reconstructions. This is because of the dorsoventrally taller squamosal in our reconstruction, as this element was broken into several pieces overlying each other, thus obscuring the full size of the element before CT scanning. As previously noted, our reconstruction resembles that of Panchen (1975) in that the squamosal extends posterior and medial to the quadratojugal to contact the quadrate, although we again note the uncertainty in this reconstruction and a potential alternate arrangement. The large gap (Fig. 3A) between the preserved anterior portion of the premaxilla and maxilla supports Smithson's (1985) reconstruction, featuring an extended premaxilla. In dorsal view, our reconstructed upper jaw features a rounded snout and widens gradually towards the jaw joints, which are the mediolaterally widest point, thus more closely resembling the reconstruction by Smithson (1985). There is a midline gap remaining between the left and right nasals and the anterior part of the frontals in our unrepaired reconstruction (Fig. 3B); however, both elements are missing their medial margins and the width of the entire skull, and of the anterior skull roof specifically, is constrained by the width of the palatal bones, the posterior skull roof bones, and articulations between the facial bones. Thus, there is strong evidence that these elements contacted their counterparts at the midline along their entire length, as in our final reconstruction (Fig. 5C). In ventral view (Fig. 3C), the anterior part of our new cranial reconstruction much more closely resembles the reconstruction by Smithson (1985) because of the wide vomers and anterior palatine, supported by information from CT data. The maxilla clearly contributes to the lateral wall of the choana, although it is still uncertain whether the premaxilla reached the choana because this element is missing its posterior portion. The outline of the subtemporal fossa is more restricted and sinuous in our new reconstruction because of the much more prominent pterygoid flange. Interestingly, the orientation of the articular surface of the quadrate in our new reconstruction is intermediate between the reconstructions by Panchen (1975) and Smithson (1985), being more anteromedially inclined in ventral view than the transversely-oriented quadrate of the former reconstruction but not to the degree of the latter reconstruction. There is a midline gap between the anterior third of the pterygoids (Fig. 3C). However, the medial margin of the anterior right pterygoid (on which the reconstruction is based) is missing; furthermore, the pterygoid medially contacts the basisphenoid and the incomplete parasphenoid posteriorly. It is likely that in life the medial margins of the pterygoids either contacted each other or a more extended cultriform process along their anterior third, forming a closed palate.

As a result of the poor contrast between bones and between bone and matrix, we could not digitally separate the bones of the posterior braincase and, therefore, do not attempt to reconstruct the occiput. However, in posterior view (Fig. 5D), our reconstruction features nearly vertically inclined sidewalls of the skull, more closely resembling the reconstruction by Panchen (1975), and the tip of the pterygoid flange projects slightly below the ventral margins of the facial skeleton. The L:W ratio of the reconstructed skull of *E. watsoni* is 1.8, narrower than the skulls of earlier tetrapods such as *Crassigyrinus* (Porro *et al*. 2023) but wider than that of *Whatcheeria* (Rawson *et al*. 2021). The new reconstruction features a H:L ratio of 0.41, a proportionately taller skull than even *Whatcheeria* (Rawson *et al*. 2021), which can be attributed to the dorsoventrally expanded squamosal and quadratojugal of *E. watsoni*; however, there is some uncertainty in this area of our reconstruction because of the missing bones of the occiput. As previously noted, the posterior margin of the upper jaw in lateral view (Fig. 5A) slopes steeply from the skull roof to the jaw joint, unlike the more gently inclined posterior skull margins of earlier tetrapods (Porro *et al*. 2015b, 2023). Maximal orbital length is 23% of total skull length (although there is some uncertainty due to breakage of the postorbital) and the orbit is nearly equal in length and height. The preorbital region (tip of the snout to anterior margin of the orbit) is 40% of total skull length while the postorbital region (posterior margin of the orbit to posterior tip of the squamosal) is 37% of total skull length – the skull of *E. watsoni* was nearly equal in length anterior and posterior to the orbit. Therefore, the postorbital region of *E. watsoni* was substantially shorter, proportionately, than the same region in *Crassigyrinus* (Porro *et al*. 2023) but longer than that of *Whatcheeria* (Rawson *et al*. 2021).

In lateral view (Fig. 4A), our 3D reconstruction of the lower jaw is gently curved, more closely resembling the overall profile of the reconstruction by Panchen (1975). The tooth-bearing region tapers gently towards the symphysis in dorsoventral height. The arrangement of bones on the lateral face resembles previous reconstructions; in medial view (Fig. 4B), however, the coronoid series and their surrounding contacts resembles the reconstruction by Smithson (1985). CT data demonstrate that the postdentary region of the jaw is strongly dorsoventrally expanded, much more so than in either of the previous reconstructions and even accounting for deformation of the specimen. The surangular crest is strongly angled as described by Smithson (1985), not gently convex as depicted by Panchen (1975) who was unable to visualise the dorsal border of the bone as it is hidden under the overlying quadratojugal. Even after removing deformation, the mandibular adductor fossa is mediolaterally narrow (Fig. 4D), its width constrained by the dentary and coronoid (anteriorly) and the surangular/articular posteriorly.

4. Discussion

4.1. New anatomical information and implications for jaw mechanics

Recent advances in medical imaging, 3D visualisation and new techniques to digitally repair fossils have revolutionised our understanding of skull anatomy and shape in early tetrapods (Porro *et al*. 2015a, 2015b, 2023; Lautenschlager *et al*. 2016; Fortuny *et al*. 2017; Ahlberg & Clack 2020; Rawson *et al*. 2021; Arbez *et al*. 2022), providing crucial new information for understanding taxonomy, phylogeny and ecology during the iconic vertebrate water–land transition. Data from µCT scans of the type specimen of *E. watsoni* provide new anatomical details of the cranium and lower jaw by revealing previously unseen internal surfaces hidden by matrix and overlying elements. We demonstrate the full extent and size of the squamosal, which was broken and obscured by overlying elements, impacting the final reconstructed shape of the skull. Additionally, we reveal the very tall surangular crest, which substantially exceeds previous reconstructions in dorsoventral height. CT scans allow us to

https://doi.org/10.1017/S175569102300018X Published online by Cambridge University Press

visualise the vomer and its teeth for the first time in *E. watsoni*, as well as confirm the presence of an elongate cultriform process of the parasphenoid. Our reconstructions of both the upper and lower jaws of *E. watsoni* are in many respects intermediate between the earlier reconstructions of Panchen (1975) and Smithson (1985); for example, scan data suggest that the squamosal may have extended medial and posterior to the quadratojugal and contacted the quadrate as suggested by Panchen (1975), but supports the shape and arrangement of the coronoid series of the lower jaw as interpreted by Smithson (1985). Finally, CT scans allow us to visualise the jaw joint morphology – particularly the articular surface of the quadrate – revealing an extensive, slightly saddle-shaped joint surface.

Although Panchen (1975) did not specifically mention a pterygoid flange in his description, he noted that the convex edge of the pterygoid descended below the jaw line in the direction of the mandibular adductor fossa. Smithson (1985) did not describe the palate in his reassessment. Both authors figured the posterior pterygoid in ventral view with a mildly convex lateral margin, forming a sinuous medial edge to the subtemporal fenestra. Scan data, in contrast, demonstrates the presence of a pronounced pterygoid flange with a rounded margin that projects well into the subtemporal fenestra (Fig. 8 and Supplementary Fig. 7D, E, F). During digital reconstruction of the skull, the palate was initially oriented horizontally (see Section 1, Material and methods). In this configuration, the pterygoid flange occluded the subtemporal fenestra and incorrectly intersected with both the surangular and quadratojugal. Vaulting of the palate resulted in the pterygoid flange being more vertically oriented, projecting below the level of the quadratojugal, and no longer intersecting either the quadratojugal or surangular.

The development of the pterygoid flange in *E. watsoni* has potentially intriguing ramifications for soft-tissue anatomy and ecology in this taxon and early tetrapods more generally. Olson (1961) first proposed that specific changes in skull shape and muscle arrangement were crucial to the development of terrestrial feeding. In particular, the skull geometry of early tetrapodomorphs (e.g., *Eusthenopteron*, *Ichthyostega*) resulted in the jaw-closing muscles being capable of exerting high force when the jaws were at a relatively wide gape, resulting in fast closure of the jaws, but a relatively weak bite with the jaws at occlusion, which Olson (1961) termed a kinetic inertial system. In contrast, more crownward tetrapods on the lineage leading to amniotes exhibit dorsoventrally taller skulls with expanded adductor chambers and mandibular adductor fossae, as well as a taller coronoid process of the lower jaw; these structural changes resulted in a static pressure system, in which the jaws exert the highest force with the tooth rows near occlusion. In particular, Olson (1961) highlighted the expansion of the transverse process of the pterygoid and the appearance of the pterygoid flange as a key step in the evolution of the amniote skull. Carroll (1969) elaborated further on the importance of the pterygoid flange, which serves as the attachment site for medial pterygoideus, stating that its appearance signalled the differentiation of the adductor muscles and acquisition of the static pressure system. These ideas have subsequently been reiterated in textbooks (Pough *et al.* 2012) and used as the basis for morphofunctional analyses of a wide range of fossil taxa (DeMar & Barghusen 1972; Taylor 1992), as well as developing further hypotheses on the forces driving and constraining skull shape during the evolution of amniotes (Janis & Keller 2001).

The presence of a pterygoid flange in *E. watsoni* represents the earliest definitive appearance of this feature of which we are aware. Smithson *et al.* (1994) noted that *Westhlothiana* from the Viséan of East Kirkton, originally considered a reptilomorph and stem amniote based on numerous characters, nonetheless lacked several amniote features including a transverse pterygoid flange. In contrast, a pterygoid flange is present in the late Carboniferous embolomere *Pholiderpeton* (Clack 1987), as well as in later and more derived seymouriamorphs and diadectomorphs (Laurin & Reisz 1995). If the pterygoid flange of *E. watsoni* represents the site of origin for medial pterygoideus (as it does in more derived tetrapods and amniotes) and can be considered a proxy for the differentiation of the jaw adductor muscles, this may indeed signal the very early development of a static pressure system in this taxon, as suggested by Smithson (1985) on the basis of jaw joint morphology (see Section 4.3, Kinesis, jaw joint and function). This in turn could indicate dietary differences between *E. watsoni* and other Carboniferous tetrapods, including the closely related and contemporary taxon *Proterogyrinus*, which does not possess a distinct pterygoid flange, as well as a more terrestrial lifestyle in *E. watsoni*, shifting towards a static pressure bite system.

An incipient pterygoid flange extending into the subtemporal fossa is also present in some temnospondyls, including *Balanerpeton* (Milner & Sequeira 1993) and members of Edopoidea (Sequeira 2003), Dissorophoidea (Milner 2018) and Archegosauroidea (Schoch & Sobral 2021). The homology between the flange found in temnospondyls and on the lineage leading to amniotes is uncertain, although recent studies have reconstructed the anterior portion of the medial adductor mandibulae internus (homologous to medial pterygoideus; also see below) in temnospondyls as originating on the interpterygoid vacuities, rather than the pterygoid flange as in amniotes (Witzmann & Werneberg 2017).

4.2. Sutural morphology

In addition to bones concealed by matrix and overlying elements, CT scanning allows visualisation of sutures, the contacts between cranial and mandibular bones. Sutures exhibit numerous different morphologies, and data from both *in vivo* bone strain experiments and biomechanical modelling have found correlations between specific suture shapes and certain loading regimes: for example, butt joints are associated with tension and bending; interdigitated sutures are associated with compression; and scarf joints are associated with complex load regimes (torsion, shear, or tension and compression) (Herring & Mucci 1991; Busbey 1995; Rafferty & Herring 1999; Herring & Teng 2000; Markey *et al.* 2006). CT scanning has permitted more recent anatomical descriptions of early tetrapods to use suture shape to predict skull load regimes – and infer the feeding strategies used to generate these loads – in several early tetrapods and extant analogues (Markey & Marshall 2007; Porro *et al.* 2015a, 2015b, 2023; Gruntmejer *et al.* 2019; Rawson *et al.* 2021).

Compared with our previous detailed descriptions of suture morphology in the skulls of early tetrapods (Porro *et al.* 2015a, 2015b, 2023; Rawson *et al.* 2021), information was more limited on the shape of contacts between individual cranial and mandibular bones in *E. watsoni*. This was for several reasons: contact areas missing entirely (i.e., nasal–nasal, postorbital–squamosal), partial or total fusion between elements (various bones of the skull table, surangular–articular), or poor scan contrast between adjacent bones (coronoid series and dentary). Nonetheless, new information was obtained from CT scans on the general distribution of different suture types in the upper and lower jaws of *E. watsoni*. The bones of the anterior snout and the sidewalls of the skull meet primarily at overlapping scarf joints, with few interdigitations present. Butt joints occur at the midline of the anterior skull roof as well as between the maxilla–jugal, maxilla–posterior portion of the lacrimal and jugal–prefrontal (Figs 3, 5). The bones of the middle and posterior skull roof join at tight contacts (except at the midline), with the marginal bones of the skull roof meeting the parietal at overlapping interdigitated contacts. The marginal palatal bones meet the premaxilla and maxilla at butt joints and are extensively underlapped by

https://doi.org/10.1017/S175569102300018X Published online by Cambridge University Press

the lateral margin of the pterygoid. The lower jaw features primarily long overlapping contacts between the bones, with the dentary meeting the splenial at a butt joint (Fig. 4). The only clear interdigitations in the lower jaw occur between the prearticular and articular, although some interdigitations may also be present between the dentary and coronoid series.

Suture morphology in the upper jaw of *E. watsoni* suggests that the anterior snout, sidewalls of the skull and the palate experienced variable and/or complex loads during feeding; this contrasts with the skull of *Crassigyrinus*, which features interdigitated sutures in the snout associated with channelling compressive stresses upwards from the teeth (Porro *et al*. 2023). Instead, the dorsoventrally taller and mediolaterally narrower skull of *E. watsoni* may have experienced more torsional and shear stresses, particularly during unilateral biting, which would have been resisted by the overlapping contacts in these regions. Overlapping sutures in the posterior part of the facial skeleton and suspensorium may have acted to resist reaction forces at the jaw joints as well as forces generated by the jaw-closing muscles. Midline butt joints in the skull roof and palate suggest these areas experienced tension during feeding, which may have been generated during unilateral biting. The skull roof features tightly interdigitated (in some cases, also overlapping) contacts to resist compressive stresses, as well as – potentially – insertion of some of the external adductor muscles as proposed for other embolomeres (Clack 1987). The lower teeth of *E. watsoni* are laterally offset from the midline of the dentary (Fig. 4D), which would have resulted in outward twisting of the mandibular ramus during biting; widespread overlapping sutures in the lower jaw would have acted to resist resulting torsional stresses, as has also been hypothesised in *Whatcheeria* (Rawson *et al*. 2021).

4.3. Kinesis, jaw joint and function

In his studies of many early tetrapods, Panchen (1972a, 1972b, 1973, 1975, 1985) suggested a mobile kinetic joint between the marginal bones of the skull roof and the bones of the upper check. Similarly, the basal articulation between the basipterygoid processes of the basisphenoid and the pterygoid has been suggested as a site that accommodated cranial kinesis in some early tetrapods (Beaumont 1977). However, Holliday & Witmer (2008) demonstrated that a seemingly mobile basal articulation occurs in many living tetrapods with akinetic skulls, and identified additional criteria – including permissive kinematic linkages and evidence of protractor muscles – necessary to infer cranial kinesis in fossil taxa.

Detailed examination of sutural shape, in many cases made possible by relatively recent application of μCT scanning, has demonstrated that cranial kinesis was unlikely in many early tetrapod taxa due to strong connections between the skull roof and facial skeleton, as in *Crassigyrinus* (Porro *et al*. 2023), as well as a lack of permissive kinematic linkages throughout the skull, as in *Acanthostega* (Porro *et al*. 2015b). However, these same methods have been used to support cranial kinesis in other early tetrapod taxa, such as *Tiktaalik* (Lemberg *et al*. 2021). As noted by Panchen (1975), the connections between the marginal bones of the skull roof and cheek of *E. watsoni* are relatively loose – the dorsal margin of the postorbital appears to have nestled into an elongate facet of the postfrontal and intertemporal whereas the lateral margins of the intertemporal and supratemporal rest on the grooved upper margin of the squamosal. This morphology does not preclude the possibility of movement between the skull roof and cheek. However, it is unclear where such movement would be accommodated elsewhere in the skull; that is, there appears to be a lack of permissive kinematic linkages. Most of the facial and palatal bones contact at overlapping scarf sutures, some of which are particularly extensive (e.g., the palatine–vomer contact). Sliding movements between elements seem unlikely; however, the skull of *E. watsoni* lacks the widespread interdigitated contacts observed in *Crassigyrinus* (Porro *et al*. 2023). Therefore, as suggested by Clack (1987) for several embolomere taxa, including *E. watsoni*, cranial kinesis seems improbable in this taxon; however, it cannot be entirely ruled out as in some other early tetrapod taxa (Porro *et al*. 2015b, 2023; Rawson *et al*. 2021).

As described by Smithson (1985) in NUZ 78.1.61, μCT scans of NMS G.1950.86.1 demonstrate that the articular surface of the jaw joint (between the quadrate and articular) faces dorsoventrally; it is neither mediolaterally nor anteroposteriorly inclined. Compared with other tetrapods, such as *Eogyrinus* (Panchen 1972a) and *Crassigyrinus* (Porro *et al*. 2023) that feature jaw joints that are strongly saddle- and screw-shaped – resulting in the dorsal (tooth-bearing) margin of the lower jaw rotating medially about its long axis during jaw closure – the jaw joint surface of *E. watsoni* is more extensive, gently saddle-shaped and not screw-shaped.

Ahlberg & Clack (1998) noted a number of features in the lower jaws of more crownward tetrapods that we identify in *E. watsoni*, including (1) the dorsolateral margin of the mandibular adductor fossa (formed by the posterior coronoid, dentary and surangular) forming a surangular crest; (2) the dorsomedial margin of the mandibular adductor fossa becoming ventrally concave, so that the fossa opens dorsomedially instead of dorsally as in earlier tetrapods; (3) lips/flanges on or ventral to the surangular crest on the posterior coronoid and surangular; and (4) lips/flanges on the prearticular on the posterior part of the fossa. Ahiberg & Clack (1998) associated all of these features as indicating differentiation of the jaw adductor muscles, in which the m. adductor mandibulae externus inserts in the area of the surangular crest and pulls the jaw posterodorsally, and the m. adductor mandibulae internus (which includes the previously mentioned medial pterygoideus [Holliday & Witmer 2007]) inserts on the prearticular and pulls anterodorsally.

Anatomical features described in the present study and in previous work give insights into skull function and potential diet in *E. watsoni*. The new 3D model agrees with previous reconstructions in having a relative dorsoventrally tall and mediolaterally narrow skull. CT scans demonstrate that overlapping scarf joints are the dominant suture type in the upper jaw; these would have resisted the torsional and shear stresses induced by twisting during biting in a dorsoventrally tall skull, particularly during unilateral biting. The extensive overlapping sutures of the lower jaw would likewise act to resist torsional and shear stresses. The simpler morphology of the jaw joint in *E. watsoni* suggests a simpler, more orthal jaw closure in this taxon than that proposed in other tetrapod species such as *Eogyrinus* (Panchen 1972a) and *Crassigyrinus* (Porro *et al*. 2023), and the orientation of the glenoid is well adapted to resist vertical joint reaction forces. The appearance of the pterygoid flange suggests differentiation of the jaw adductor musculature into external and internal components, as suggested by previous authors (Olson 1961; Carroll 1969; Clack 1987), as does the reorientation of the mandibular adductor fossa, presence of a surangular crest, and potential attachment areas for the jaw adductors on the posterior coronoid, surangular and prearticular (Ahlberg & Clack 1998). Based on these anatomical characteristics – as well as the size and shape of the dentition and absence of the lateral line – Smithson (1985) suggested that *E. watsoni* used an early static pressure system in which bite force is greatest with the jaws at or near occlusion to consume primarily terrestrial invertebrate and small vertebrate prey. Clack (1987), however, observed that the two jaw-closing systems (kinetic inertial and static pressure) proposed by Olson (1961) were potentially oversimplified, and that some early tetrapods such as *Pholiderpeton* may have possessed muscles that permitted some degree of

https://doi.org/10.1017/S175569102300018X Published online by Cambridge University Press

both jaw-closing systems – that is, fast jaw closure from a wide gape as well as a strong bite with the jaws near occlusion. Thus, *E. watsoni* and its closest relatives may represent crucial transitional forms – in terms of feeding apparatus – in the vertebrate conquest of terrestrial environments.

5. Conclusions

CT scanning and 3D visualisation have revealed new anatomical details of the skull of the transitional Carboniferous tetrapod *Eoherpeton watsoni*, enabling the first description of the tooth-bearing vomer, detailed morphology of the basipterygoid and jaw joints, the full extent of the pterygoid flange and surangular crest, and sutural morphology of the upper and lower jaws. The digitally reconstructed 3D cranium and lower jaw resemble previous attempts, with similarities to reconstructions by both Panchen (1975) and Smithson (1985). Evidence from upper and lower jaw shape, sutural morphology, jaw joint shape and osteological correlates of jaw adductor musculature all suggest *E. watsoni* used a static pressure jaw mechanism (or possibly an intermediate between a kinetic inertial and static pressure system) with more vertically oriented jaw joint reaction forces to hunt and consume terrestrial prey, hypotheses that will be tested further through biomechanical modelling.

6. Supplementary material

Supplementary material is available online at https://doi.org/10.1017/S175569102300018X.

7. Acknowledgements

This paper is dedicated to our colleague and friend Tim Smithson, who over the years has shared his extensive knowledge of Carboniferous tetrapods with us and so many other colleagues, and who has contributed immensely to our knowledge of *Eoherpeton*. Many thanks to Stig Walsh (National Museums Scotland) for access to and providing photographs of the type specimen, Dan Sykes (Natural History Museum, London) for µCT scanning, Alejandra Sánchez-Eróstegui and Jean Luc Garnier (Thermo Fisher Scientific) for providing technical support for Avizo/Amira, and our colleagues on the early tetrapod project Hugo Dutel and James Rawson for their support. This work was funded by the Natural Environment Research Council Standard Grant NE/P013090/1 to E. J. Rayfield, M. J. Fagan and L. B. Porro and Marie Curie International Incoming Research Fellowship ('Tetrapods Rising', 303161) to L. B. Porro.

8. Competing interests

The authors declare none.

9. References

Ahlberg, P. E. & Clack, J. A. 1998. Lower jaws, lower tetrapods – a review based on the Devonian genus *Acanthostega*. *Transactions of the Royal Socity of Edinburgh: Earth Sciences* **89**, 11–46.

Ahlberg, P. E. & Clack, J. A. 2020. The smallest known Devonia tetrapod shows unexpectedly derived features. *Royal Society Open Science* **7**, 1–10. doi: 10.1098/rsos.192117

Ahlberg, P. E. & Milner, A. R. 1994. The origin and early diversification of tetrapods. *Nature* **368**, 507–14.

Anderson, P. S. L., Friedman, M. & Ruta, M. 2013. Late to the table: diversification of tetrapod mandibular mechanics lagged behind the evolution of terrestriality. *Integrative and Comparative Biology* **53**, 197–208.

Arbez, T., Atkins, J. B. & Maddin, H. C. 2022. Cranial anatomy and systematics of *Dendrerpeton cf. helogenes* (Tetrapoda, Temnospondyli) from the Pennsylvanian of Joggins, revisited through micro-CT scanning. *Papers in Palaeontology* **8**, e1421. doi: 10.1002/spp2.1421

Beaumont, E. I. 1977. Cranial morphology of the Loxommatidae (Amphibia: Labyrinthodontia). *Philosophical Transactions of the Royal Society of London. B, Biological Sciences* **280**, 29–101.

Boisvert, C. A., Makr-Kurik, E. &Ahlberg, P. E. 2008. The pectoral fin of *Panderichthys* and the origin of digits. *Nature* **456**, 636–8.

Bolt, J. R. & Lombard, R. E. 2018. Palate and braincase of *Whatcheeria deltae* Lombard and Bolt. *Earth and Environmental Science Transactions of the Royal Society of Edinburgh* **109**, 177–200.

Busbey, A. P. 1995. The structural consequences of skull flattening in crocodilians. In Thomason, J. J. (ed.) *Functional Morphology in Vertebrate Paleontology*, 173–92. Cambridge: Cambridge University Press, 293.

Carroll, R. L. 1969. Problems of the origin of reptiles. *Biological Reviews* **44**, 393–432.

Clack, J. A. 1987. *Pholiderpeton scutigerum* Huxley, an amphibian from the Yorkshire coal measures. *Philosophical Transactions of the Royal Society of London. B, Biological Sciences* **318**, 1–107.

Clack, J. A. 2006. The emergence of early tetrapods. *Palaeogeography, Palaeoclimatology, Palaeoecology* **232**, 167–89.

Clack, J. A. 2009. The fin to limb transition: new data, interpretations, and hypotheses from paleontology and developmental biology. *Annual Review of Earth and Planetary Sciences* **37**, 163–79.

Clack, J. A. 2012. *Gaining Ground: The Origin and Evolution of Tetrapods*. Bloomington, Indiana, USA: Indiana University Press.

Clack, J. A. & Holmes, R. 1988. The braincase of the anthracosaur *Archeria crassidisca* with comments on the interrelationships of primitive tetrapods. *Palaeontology* **31**, 85–107.

Conroy, G. C. & Vannier, M. W. 1984. Noninvasive three-dimensional computer imaging of matrix-filled fossil skulls by high-resolution computed tomography. *Science (New York, N.Y.)* **226**, 456–8.

Cunningham, J. A., Rahman, I. A., Lautehschlager, S., Rayfield, E. J. & Donoghue, P. C. J. 2014. A virtual world of paleontology. *Trends in Ecology and Evolution* **29**, 347–57.

Daeschler, E. B., Shubin, N. H. & Jenkins Jr. F. A. 2006. A Devonian tetrapod-like fish and the evolution of the tetrapod body plan. *Nature* **440**, 757–63.

Davis, P. R. & Napier, J. 1963. A reconstruction of the skull of *Proconsul africanus* (R.S. 51). *Folia Primatologica* **1**, 20–8.

Deakin, W. J., Anderson, P. L., Boer, W. D., Smith, T. J., Hill, J. J., Rücklin, M., Donoghue, P. C. J. & Rayfield, E. J. 2022. Increasing morphological disparity and decreasing optimality for jaw speed and strength during the radiation of jawed vertebrates. *Science Advances* **8**, eabl3644. doi: 10.1126/sciadv.abl3644

DeMar, R. & Barghusen, H. R. 1972. Mechanics and the evolution of the synapsid jaw. *Evolution* **26**, 622–37.

Demuth, O. E., Wiseman, A. L. A. & Hutchinson, J. R. 2023. Quantitative biomechanical assessment of locomotor capabilities in the stem archosaur *Euparkeria capensis*. *Royal Society Open Science* **10**, 221195.

Felice, R. N., Watanabe, A., Cuff, A. R., Hanson, M., Bhullar, B.-A. S., Rayfield, E. R., Witmer, L. M., Norell, M. A. & Goswami, A. 2020. Decelerated dinosaur skull evolution with the origin of birds. *PLoS Biology* **18**, e3000801.

Fortuny, J., Marce-Nogue, J. & Konietzko-Meier, D. 2017. Feeding biomechanics of Late Triassic metoposaurids (Amphibia : Temnospondyli): a 3D finite element analysis approach. *Journal of Anatomy* **230**, 752–65.

Graham, J. B., Wegner, N. C., Miller, L. A., Jew, C. J., Chin Lai, N., Berquist, R. M., Frank, L. R. & Long, J. A. 2014. Spiracular air breathing in polypterid fishes and its implications for aerial respiration in stem tetrapods. *Nature Communications* **5**, 3022.

Gruntmejer, K., Konietzko-Meier, D., Marcé-Nogué, J., Bodzioch, A. & Fortuny, J. 2019. Cranial suture biomechanics in *Metoposaurus krasiejwensis* (Temnospondyli, Stereospndyli) from the upper Triassic of Poland. *Journal of Morphology* **280**, 1850–64.

Gunz, P., Mitteroecker, P., Neubauer, S., Weber, G. W. & Bookstein, F. L. 2009. Principles for the virtual reconstruction of hominin crania. *Journal of Human Evolution* **57**, 48–62.

Heiss, E., Aerts, P. & Van Wassenbergh, S. 2018. Aquatic transitions of feeding systems n vertebrates: a mechanical perspective. *Journal of Experimental Biology* **221**, jeb154427.

Herring, S. W. & Mucci, R. J. 1991. *In vivo* strain in cranial sutures: the zygomatic arch. *Journal of Morphology* **207**, 225–39.

Herring, S. W. & Teng, S. 2000. Strain in the braincase and its sutures during function. *American Journal of Physical Anthropology* **112**, 575–93.

Holliday, C. M. & Witmer, L. M. 2007. Archosaur adductor chamber evolution: integration of musculoskeletal and topological criteria in jaw muscle homology. *Journal of Morphology* **268**, 457–549.

Holliday, C. M. & Witmer, L. M. 2008. Cranial kinesis in dinosaurs: intracranial joints, protractor muscles, and their significance for cranial evolution and function in dinosaurs. *Journal of Vertebrate Paleontology* **28**, 1073–88.

Huxley, T. H. 1862. On new labyrinthodonts from the Edinburgh Coalfield. *Quarterly Journal of the Geological Society London* **18**, 291–6.
Janis, C. M. & Farmer, C. 1999. Proposed habitats of early tetrapods: gills, kidneys, and the water-land transition. *Zoological Journal of the Linnean Society* **126**, 117–26.
Janis, C. M. & Keller, J. C. 2001. Modes of ventilation in early tetrapods: costal aspiration as a key feature of amniotes. *Acta Palaeontologica Polonica* **46**, 137–70.
Klembara, J., Clack, J. A. & Cernansky, A. 2010. The anatomy of the palate of *Chroniosaurus dongusensis* (Chroniosuchia, Chroniosuchida) from the Upper Permian of Russia. *Palaeontology* **53**, 1147–53.
Laurin, M., Girondot, M. & De Ricqlès, A. 2000. Early tetrapod evolution. *Trends in Ecology and Evolution* **15**, 118–23.
Laurin, M. & Reisz, R. R. 1995. A reevaluation of early amniote phylogeny. *Zoological Journal of the Linnean Society* **113**, 165–223.
Lautenschlager, S. 2016. Reconstructing the past: methods and techniques for the digital restoration of fossils. *Royal Society Open Science* **3**, 160342.
Lautenschlager, S. 2017. From bone to pixel – fossil restoration and reconstruction with digital techniques. *Geologu Today* **33**, 155–9.
Lautenschlager, S., Witzmann, F. & Werneburg, I. 2016. Palate anatomy and morphofunctional aspects of interpterygoid vacuities in temnospondyl cranial evolution. *Naturwissenschaften* **103**, 79.
Lemberg, J. B., Daeschler, E. B. & Shubin, N. H. 2021. The feeding system of *Tiktaalik rosae:* an intermediate between suction feeding and biting. *Proceedings of the National Academy of Sciences* **118**, e2016421118. doi: 10.1073/pnas.201642118
Markey, M. J., Main, R. P. & Marshall, C. D. 2006. *In vivo* cranial suture function and suture morphology in the extant fish *Polypterus:* implications for inferring skull function in living and fossil fish. *Journal of Experimental Biology* **209**, 2085–102.
Markey, M. J. & Marshall, C. R. 2007. Terrestrial-style feeding in a very early aquatic tetrapod is supported by evidence from experimental analysis of suture morphology. *Proceedings of the National Academy of Sciences of the United States of America* **104**, 7134–8.
Milner, A. R. 2018. Two primitive trematopid amphibians (Temnospondyli, Dissorophoidea) from the Upper Carboniferous of the Czech Republic. *Earth and Environmental Sciences Transactions of the Royal Society of Edinburgh* **109**, 201–23.
Milner, A. R. & Sequeira, S. E. K. 1993. The temnospondyl amphibians from the Viséan of East Kirkton, West Lothian, Scotland. *Transactions of the Royal Society of Edinburgh: Earth Sciences* **84**, 331–61.
Molnar, J. L., Diogo, R., Hutchinson, J. R. & Pierce, S. E. 2018. Reconstructing pectoral appendicular muscle anatomy in fossil fish and tetrapods over the fins-to-limbs transition. *Biological Reviews* **93**, 1077–107.
Motani, R. 1997. New technique for retrodeforming tectonically deformed fossils, with an example for ichthyosaurian specimens. *Lethaia* **30**, 221–8.
Neenan, J. M., Ruta, M., Clack, J. A. & Rayfield, E. J. 2014. Feeding biomechanics in *Acanthostega* and across the fish–tetrapod transition. *Proceedings of the Royal Society B: Biological Sciences* **281**, 20132689.
Olson, E. C. 1961. Jaw mechanisms: rhipidistians, amphibians, reptiles. *American Zoologist* **1**, 205–15.
Panchen, A. L. 1972a. The skull and skeleton of *Eogyrinus attheyi* Watson (Amphibia: Labyrinthodontia). *Philosophical Transactions of the Royal Society of London. B, Biological Sciences* **263**, 279–326.
Panchen, A. L. 1972b. The interrelationships of the earliest tetrapods. In Joysey, K. A & Kemp, T. S. (eds) *Studies in Vertebrate Evolution – Essays Presented to Dr. F. R. Parrington, F.R.S.*, 65–87. Edinburgh: Oliver & Boyd.
Panchen, A. L. 1973. On *Crassigyrinus scoticus* Watson, a primitive amphibian from the Lower Carboniferous of Scotland. *Palaeontology* **16**, 179–93.
Panchen, A. L. 1975. A new genus and species of anthracosaur amphibian from the Lower Carboniferous of Scotland and the status of *Pholidogaster pisciformis* Huxley. *Philosophical Transactions of the Royal Society of London. B, Biological Sciences* **269**, 581–637.
Panchen, A. L. 1985. On the amphibian *Crassigyrinus scoticus* Watson from the Carboniferous of Scotland. *Philosophical Transactions of the Royal Society of London. B, Biological Sciences* **309**, 505–68.
Pardo, J. D. & Anderson, J. S. 2016. Cranial morphology of the Carboniferous-Permian tetrapod *Brachydectes newberryi* (Lepospondyli, Lysorophia): new data from μCT. *PLoS ONE* **11**, e0161823. doi: 10.1371/journal.pone.0161823
Pardo, J. D., Szostakiwskyj, M., Ahlberg, P. E. & Anderson, J. S. 2017. Hidden morphological diversity among early tetrapods. *Nature* **546**, 642–5.
Pierce, S. E., Clack, J. A. & Hutchinson, J. R. 2012. Three-dimensional limb joint mobility in the early tetrapod *Ichthyostega*. *Nature* **486**, 523–6.
Porro, L. B., Rayfield, E. J. & Clack, J. A. 2015a. Computed tomography, anatomical description and three-dimensional reconstruction of the lower jaw of *Eusthenopteron foordi* Whiteaves, 1881 from the Upper Devonian of Canada. *Palaeontology* **58**, 1031–47.
Porro, L. B., Rayfield, E. J. & Clack, J. A. 2015b. Descriptive anatomy and three-dimensional reconstruction of the skull of the early tetrapods *Acanthostega gunnari* Jarvik, 1952. *PLoS ONE* **10**, e0124731. doi: 10.1371/journal.pone.0124731
Porro, L. B., Rayfield, E. J. & Clack, J. A. 2023. Computed tomography and three-dimensional reconstruction of the skull of the stem tetrapod *Crassigyrinus scoticus* Watson, 1929. *Journal of Vertebrate Paleontology* **42**, 1–31. doi: 10.1080/02724634.2023.2183134
Pough, F. H., Janis, C. M. & Heiser, J. B. 2012. *Vertebrate Life*. London, UK: Pearson, 720 pp.
Rafferty, K. L. & Herring, S. W. 1999. Craniofacial sutures: morphology, growth, and *in vivo* masticatory strain. *Journal of Morphology* **242**, 167–79.
Rahman, I. A. & Smith, S. Y. 2014. Virtual paleontology: computer-aided analysis of fossil form and function. *Journal of Palaeontology* **88**, 633–5.
Rawson, J. R. G., Porro, L. B., Martin-Silverstone, E. & Rayfield, E. J. 2021. Osteology and digital reconstruction of the skull of the early tetrapod *Whatcheeria deltae*. *Journal of Vertebrate Paleontology* **41**, e1927749. doi: 10.1080/02724634.2021.1927749
Rayfield, E. J. 2007. Finite element analysis and understanding the biomechanics and evolution of living and fossil organisms. *Annual Review of Earth and Planetary Sciences* **35**, 541–76.
Romer, A. S. 1963. The larger embolomerous amphibians of the American Carboniferous. *Bulletin of the Museum of Comparative Zoology* **128**, 415–54.
Romer, A. S. 1970. A new anthracosaurian labyrinthodont, *Proterogyrinus scheelei*, from the Lower Carboniferous. *Kirtlandia* **10**, 1–16.
Rosen, D. E., Forey, P. L., Gardiner, B. G. & Patterson, C. 1981. Lungfishes, tetrapods, paleontology, and plesiomorphy. *Bulletin of the American Museum of Natural History* **167**, 159–276.
Schoch, R. R. & Sobral, G. 2021. A new species of *Sclerocephalus* with a fully ossified endocranium gives insight into braincase evolution in temnospondyls. *Journal of Paleontology* **95**, 1308–20.
Sequeira, S. E. K. 2003. The skull of *Cochleosaurus bohemicus* Frič, a temnospondyl from the Czech Republic (Upper Carboniferous) and cochleosaurid relationships. *Transactions of the Royal Society of Edinburgh: Earth Sciences* **94**, 21–43.
Shubin, N. H., Daeschler, E. B. & Jenkins, F. A. 2006. The pectoral fin of *Tiktaalik roseae* and the origin of the tetrapod limb. *Nature* **440**, 764–71.
Smithson, T. R. 1980. An early tetrapod fauna from the Namurian of Scotland. In Panchen, A. L. (ed.) *The Terrestrial Environment and the Origin of Land Vertebrates*, 407–38. London, UK: Academic Press London 633 pp.
Smithson, T. R. 1985. The morphology and relationships of the Carboniferous amphibian *Eoherpeton watsoni* Panchen. *Zoological Journal of the Linnean Society* **85**, 317–410.
Smithson, T. R., Carroll, R. L., Panchen, A. L. & Andrews, S. M. 1994. *Westlothiana lizziae* from the Viséan of East Kirkton, West Lothian, Scotland, and the amniote stem. *Transactions of the Royal Society of Edinburgh: Earth Sciences* **84**, 383–412.
Taylor, M. A. 1992. Functional anatomy of the head of the large aquatic predator *Rhomaleosaurus zetlandicus* (Plesiosauria, Reptilia) from the Toarcian (Lower Jurassic) of Yorkshire, England. *Philosophical Transactions: Biological Sciences* **1274**, 247–80.
Van Wassenberg, S. 2019. Transitions from water to land: terrestrial feeding in fishes. In Bels, V. & Whishaw, I. G. (eds.) *Feeding in Vertebrates: Morphology, Behaviour, Biomechanics*, 139–58. New York City, New York, USA: Springer 1092 pp.
Wainwright, P. C., McGee, M. D., Longo, S. L. & Hernandez, L. P. 2015. Origins, innovations and diversification of suction feeding in vertebrates. *Integrative and Comparative Biology* **55**, 134–45.
Watson, D. M. S. 1929. The Carboniferous Amphibia of Scotland. *Palaeontologia Hungarica* **1**, 219–52.
Witzmann, F. & Werneberg, I. 2017. The palatal interpterygoid vacuities of temnospondyls and the implications for the associated eye- and jaw musculature. *The Anatomical Record* **300**, 1240–69.
Zollikofer, C. P. E., Ponce de Leon, M. S., Martin, R. D. & Stucki, P. 1995. Neanderthal computer skulls. *Nature* **375**, 283–5.

MS received 1 April 2023. Accepted for publication 27 November 2023